Controls on Phosphorus Mobility in the Potomac River Near the Blue Plains Wastewater Treatment Plant

By PAUL P. HEARN, Jr.

U.S. GEOLOGICAL SURVEY WATER-SUPPLY PAPER 2231

UNITED STATES DEPARTMENT OF THE INTERIOR
WILLIAM P. CLARK, Secretary

GEOLOGICAL SURVEY
Dallas L. Peck, Director

UNITED STATES GOVERNMENT PRINTING OFFICE: 1985

For sale by Distribution Branch
Text Products Section
U.S. Geological Survey
604 South Pickett Street
Alexandria, Virginia 22304

Library of Congress Cataloging in Publication Date

Hearn, Paul P., Jr
Controls on phosphorus mobility in the Potomac River near the Blue Plains Wastewater Treatment Plant

(Geological Survey water-supply paper ; 2231)
Bibliography: p.
Supt. of Docs. no.: I 19.13:2231
1. Water—Phosphorus content. 2. Sediment transport—Potomac River Watershed. 3. Water chemistry. 4. Water—Pollution—Potomac River Watershed. I. Title. II. Title: Blue Plains Wastewater Treatment Plant
TD427.P56H43 1984 628.1'682 83-200378

CONTENTS

APPENDIXES

FIGURES

TABLES

Controls on Phosphorus Mobility in the Potomac River Near the Blue Plains Wastewater Treatment Plant

By Paul P. Hearn, Jr.

Abstract

The Blue Plains wastewater treatment plant is the largest point source of phosphorus in the Potomac River basin, discharging an average of 2 metric tons of phosphorus into the river each day in 1980. An intensive study of the water and sediments in the vicinity of the treatment plant was conducted in 1979–80 in order to characterize the major factors controlling the mobility of effluent-derived phosphorus in the area.

The transport of phosphorus near the treatment plant was found to be affected by the circulation regime, by inorganic adsorption reactions with sediments, and by metabolic uptake and release by phytoplankton. The effect of river discharge on the convective transport of phosphorus near the outfall is significantly reduced by a midriver shoal area, which confines the flow path of the effluent to an embayment on the eastern side of the river for a distance of 4 kilometers below the outfall. This embayment appears to serve as a sediment trap, where protection from bottom scour during high-flow events has permitted fine-grained sediments to accumulate. Measurements of mean residence time indicate that the effluent leaves the embayment area 2½ days after being discharged from the outfall.

Measurements of the linear decay constant for the removal of dissolved phosphorus from the water column reveal a diurnal cycle corresponding to the metabolic utilization of phosphorus by phytoplankton. This cyclic removal is superimposed on a constant and noncyclic adsorption of phosphorus by inorganic phases. Forty-eight hour average values of the linear decay constant for dissolved phosphorus in the area range from 0.4 to 1.1 per day.

Analyses of bottom sediments indicate that approximately 13 percent of the phosphorus discharged between September 1977 and August 1980 has been retained in the embayment. The primary inorganic phase responsible for phosphorus adsorption is amorphous iron (ferric oxy-hydroxides); amorphous aluminum and clay minerals appear to play secondary roles. The accumulation of sorbed phosphorus in the embayment has been promoted by the deposition of fine-grained sediments enriched in ferric oxy-hydroxides. Conversely, the absence of ferric oxy-hydroxides in coarse-grained sediments near the outfall has facilitated the precipitation of the ferrous phosphate mineral vivianite.

INTRODUCTION

While phosphorus is an essential nutrient in aquatic ecosystems, it is also a major cause of eutrophication when concentrations exceed critical levels. The rapid growth of planktonic algae in response to increased phosphorus loadings has been a common occurrence in lakes, rivers, and estuaries where the discharge of sewage or runoff from fertilized fields has disturbed the natural equilibrium. Uncontrolled algal growth can affect the quality of domestic water supplies, damage fisheries, and spoil recreational areas. From the standpoint of safeguarding pulic health as well as protecting a valuable economic resource, the control of eutrophication is of paramount importance.

The removal of phosphorus from wastewater treatment plant effluents has become increasingly desirable, both in terms of positive effects on water quality and also because of the lower costs relative to the removal of nitrogen or carbon. Unfortunately, planners responsible for deciding whether removal is warranted often have only limited information regarding the nature of the body of water receiving the effluent.

Once phosphorus is introduced into a river, lake, or estuary, its availability to photosynthesizing organisms is controlled by several complex and time-variable processes. Before the the behavior of phosphorus in a given environment can be predicted with any certainty, the nature and relative importance of each component process must be understood. This paper will characterize the major factors controlling the mobility of phosphorus discharged into the Potomac River by the Blue Plains sewage treatment plant, the largest point source of this nutrient in the Potomac River basin.

Study Area

The Blue Plains wastewater treatment plant is located in the District of Columbia, on the eastern side of the Potomac River near the border between the District of Columbia and the State of Maryland (fig. 1). During the last half of the 19th century, the only treatment given to domestic wastes from the District of Columbia was simple dilution provided by the Potomac River. Discharges in excess of the assimilative capacity of the river resulted in offensive conditions along the waterfront and posed a serious health hazard to the local population. To cope with this problem, a sewerage system was installed to divert waste to a point far enough downriver to prevent its return by tidal action. This arrangement was satisfactory until the early 1930's, when the need for a treatment facility was recognized. Construction on the plant at Blue Plains was begun in 1935, and the plant was first put into operation in 1938. The original facilities were enlarged and upgraded in the early fifties; modifications and improvements continued in the seventies. The main outfall was enlarged and relocated from its previous location in the main channel to its current site (see fig. 1) in September 1977 (Ed Jones, personal commun.).

The Blue Plains plant currently receives influent from 725 square miles of tributary area in the District of Columbia, Maryland, and Virginia (fig. 2). Routinely processing flows in excess of 300 million gallons per day, Blue Plains is one of the largest advanced wastewater treatment plants in the world (Schwinn and Tozer, 1974).

Plan of Study

The major objective of the study was the characterization of the chemical, biological, and physical processes influencing the transport of phosphorus discharged into the Potomac River by the Blue Plains treatment plant. Work was designed to take place in two stages. The first stage involved a slug injection of dye tracer to map the flow path of the effluent, and preliminary water sampling to establish the general distribution of dissolved phosphorus. These data were used in planning subsequent sampling. The second stage involved the collection of gravity cores for analysis of sediments and associated interstitial waters, and a 1 tidal-day dye injection followed by 6 days of continuous water-column sampling to determine the residence time of the effluent and to measure the decay constant for dissolved phosphorus in the area.

ACKNOWLEDGMENTS

This work would not have been possible without the help of numerous USGS personnel, who were generous in offering both their advice and their assistance. Ted Callender, Ron Cohen, Steve Goodwin, Dan Hahl, Ward Hickman, Mary Mrose, David Parkhurst, Liz Piercey, Barbara Shultz, Nancy Simon, Ellen Spaulding, Nobuhiro Yotsukura, and Wayne Webb all contributed to various aspects of the study. Their help is gratefully acknowledged.

METHODS

Water-Column Sampling Techniques

September 1979 Study

Depth-integrated water samples were collected four times over a single tidal cycle at each of 13 sites (fig. 3). By using four boats, all 13 sites were occupied within 20 minutes of each other. Samples were pumped at a continuous rate with a battery-operated peristaltic pump and were depth integrated by raising the collection hose from the bottom to the surface at a constant rate.

Following each collection interval, samples were taken to a U.S. Geological Survey laboratory facility at the nearby Alexandria (Va.) Coast Guard station. There the samples were filtered through preweighed 0.45- m membrane filters (Millipor type HA), and the filtrates were refrigerated.

August 1980 Study

Time-series water-column samples were collected continuously over a 6-day period using an array of six automatic sampler boats (fig. 4). The boats were originally designed to collect water samples for dye tracer studies (Kilpatrick, 1972). Each sampler contains 24 spring-loaded, 25-ml polyethylene syringes, which are triggered sequentially by a battery-operated mechanism. By changing the combination of gears in the drive mechanism, it is possible to vary the sampling interval from 50 to 120 minutes. The syringes and timing mechanism are contained in an aluminum box, which is housed in a Styrofoam-filled fiberglass shroud for flotation. The syringe array is easily removed from the fiberglass shroud, so the shroud can be left on its mooring line while the syringes are being retrieved. The sampler mechanism and the fiberglass flotation shroud are illustrated in figure 5.

A timing interval of 50 minutes was used for the first 80 hours of sampling, and a 120-minute interval was used for the remainder of the study. Samples for the

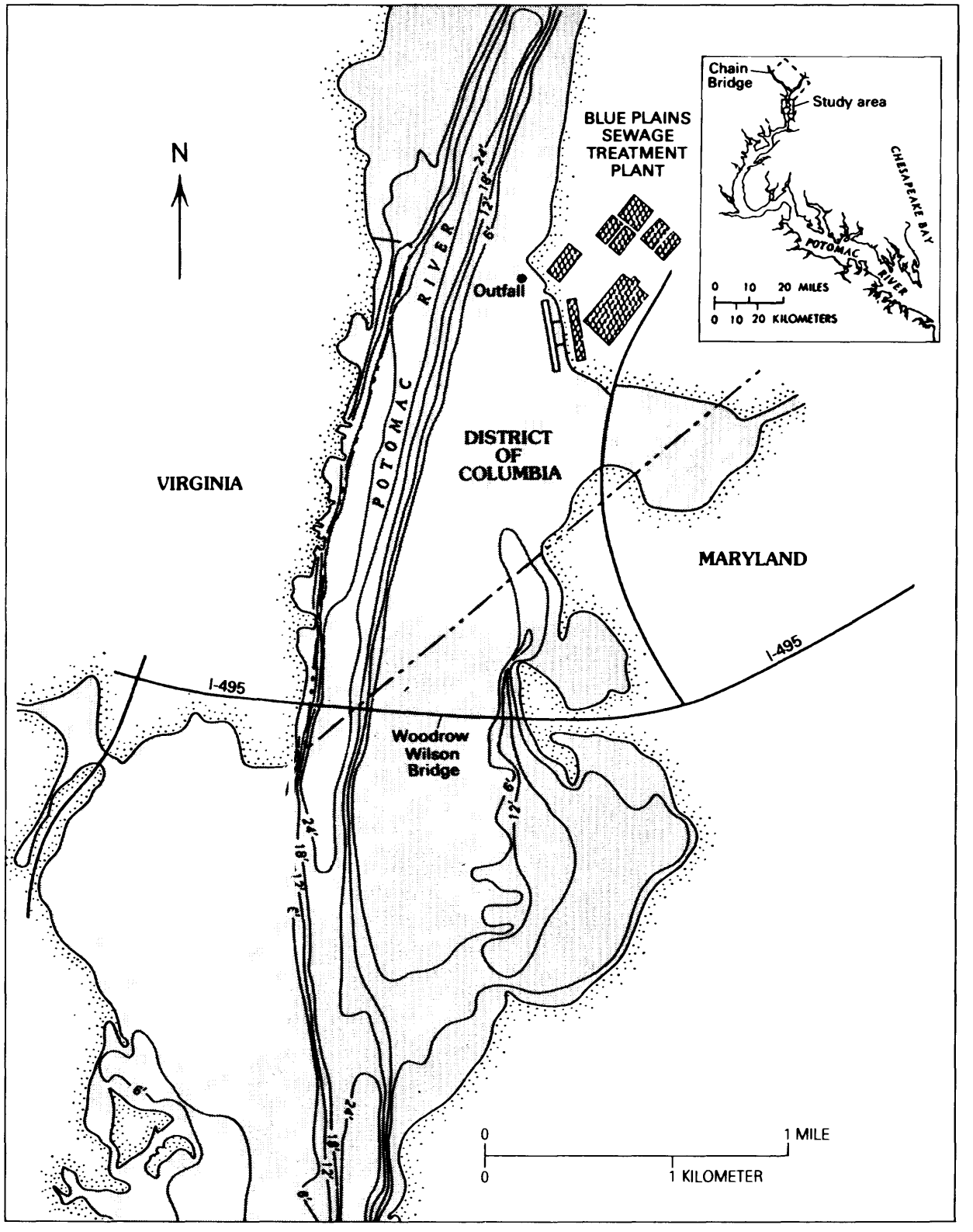

Figure 1. Location of Blue Plains sewage treatment plant and bathymetric contours in the Potomac River.

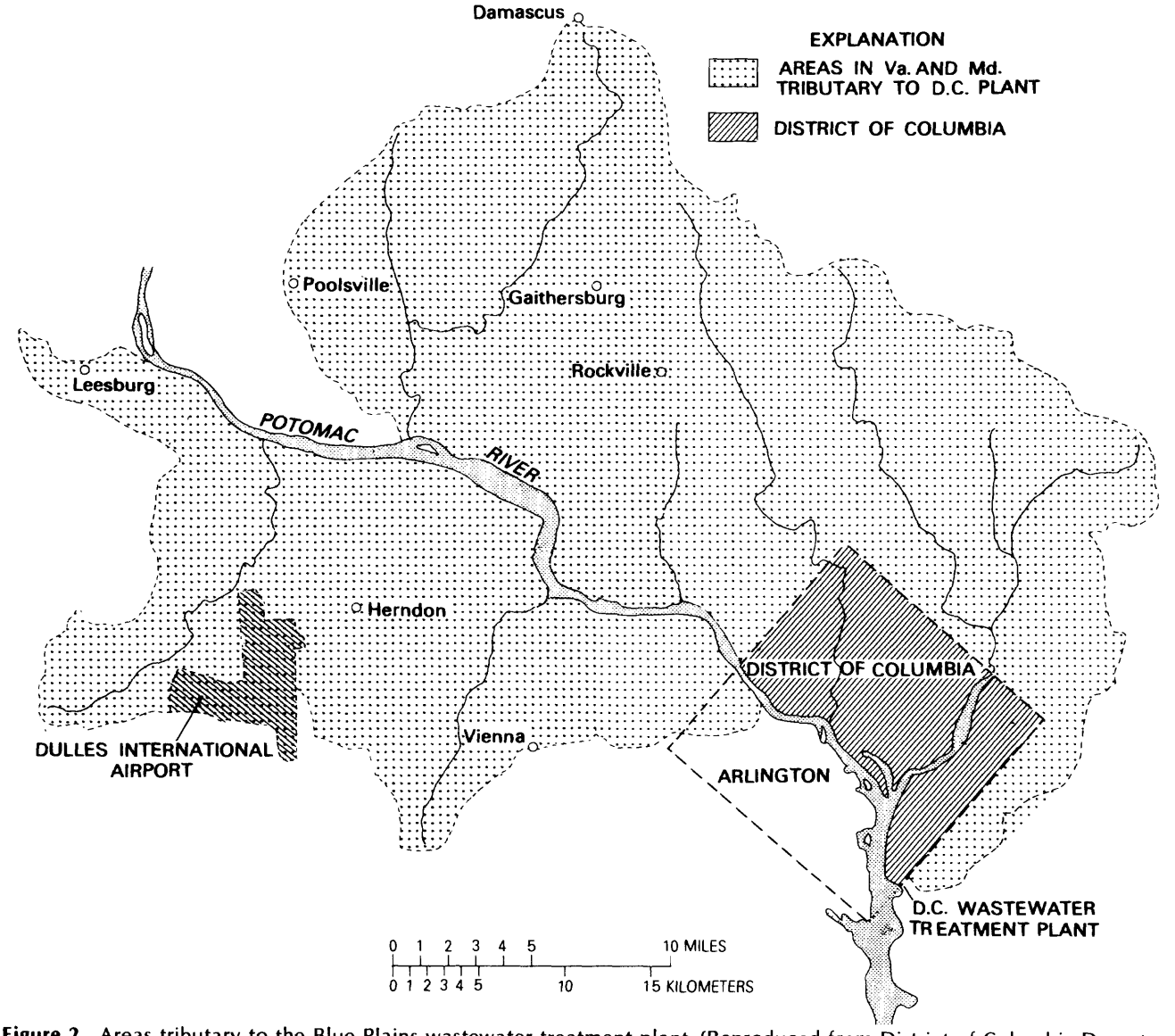

Figure 2. Areas tributary to the Blue Plains wastewater treatment plant. (Reproduced from District of Columbia Department of Environmental Services Brochure ES-6).

determination of dissolved phosphorus, chloride, and dye concentration were collected during the first 60 hours of the study. Samples for dye determination alone were collected during the remainder of the study. Samplers were unloaded and reloaded with fresh syringes every 20 or 48 hours, depending on the sampling interval. Syringes were capped to prevent leakage, placed in specially constructed racks to minimize movement, and taken to the laboratory at the Alexandria Coast Guard station for processing.

Immediately after arriving at the laboratory, samples were filtered through 0.45-μm-pore-size, 25-mm nitrocellulose filters (Millipore type HA). To simplify sample handling and to reduce the amount of loss, a graduated cylinder was fitted into the system to receive the filtrate. This made it possible to empty the entire contents of each syringe into the filter funnel, read the volume of filtrate passing the filter into the graduated cylinder, and then transfer the filtrate to a separate labeled vial.

Bottom Sediment Sampling Techniques

Samples of bottom sediments were obtained by taking short cores at several points within the study area. All cores were collected by free fall with a gravity coring device or by direct insertion with an extender

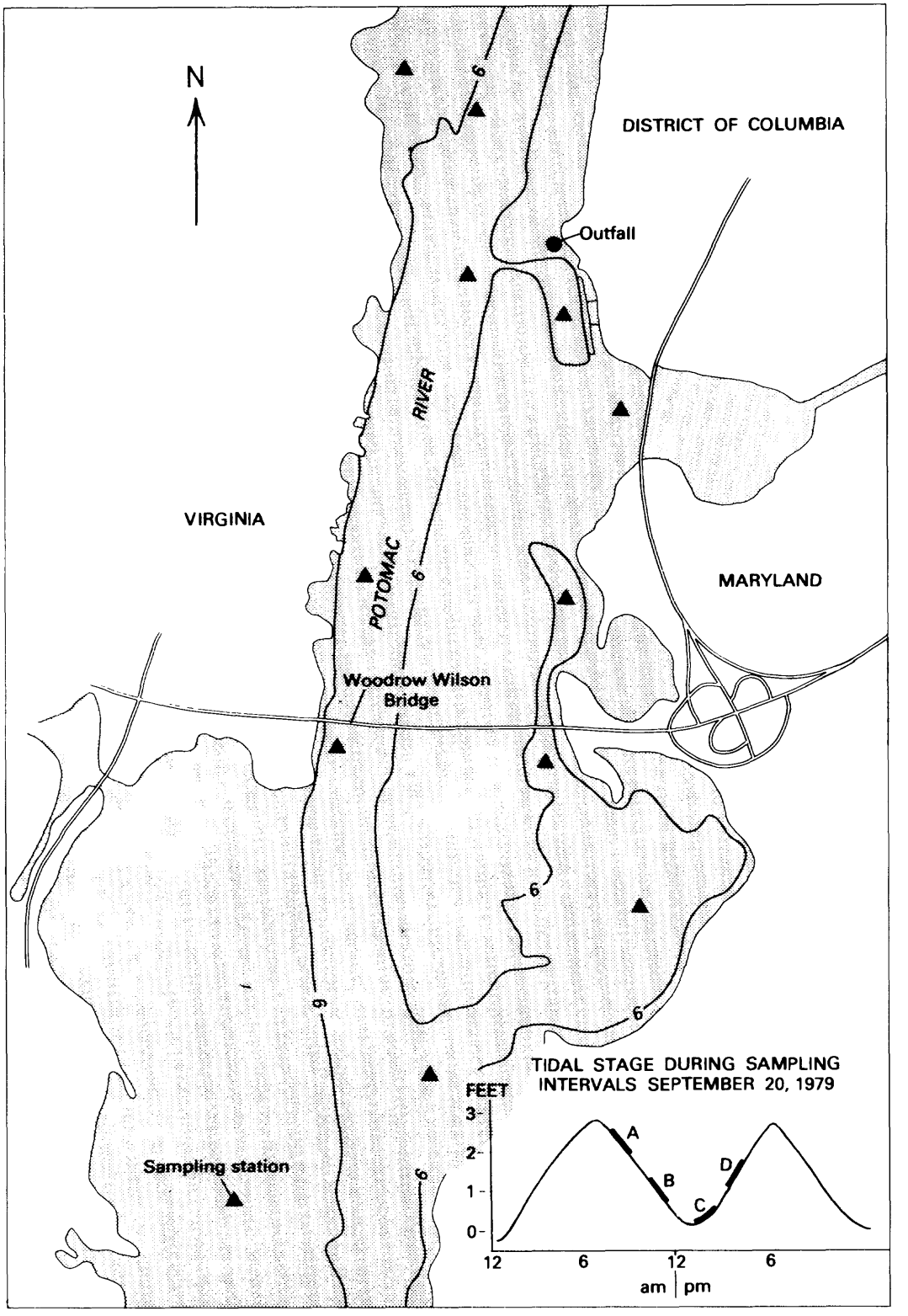

Figure 3. Water-column sampling stations for the September 1979 study. Six-foot depth contour indicates configuration of main channel and embayment.

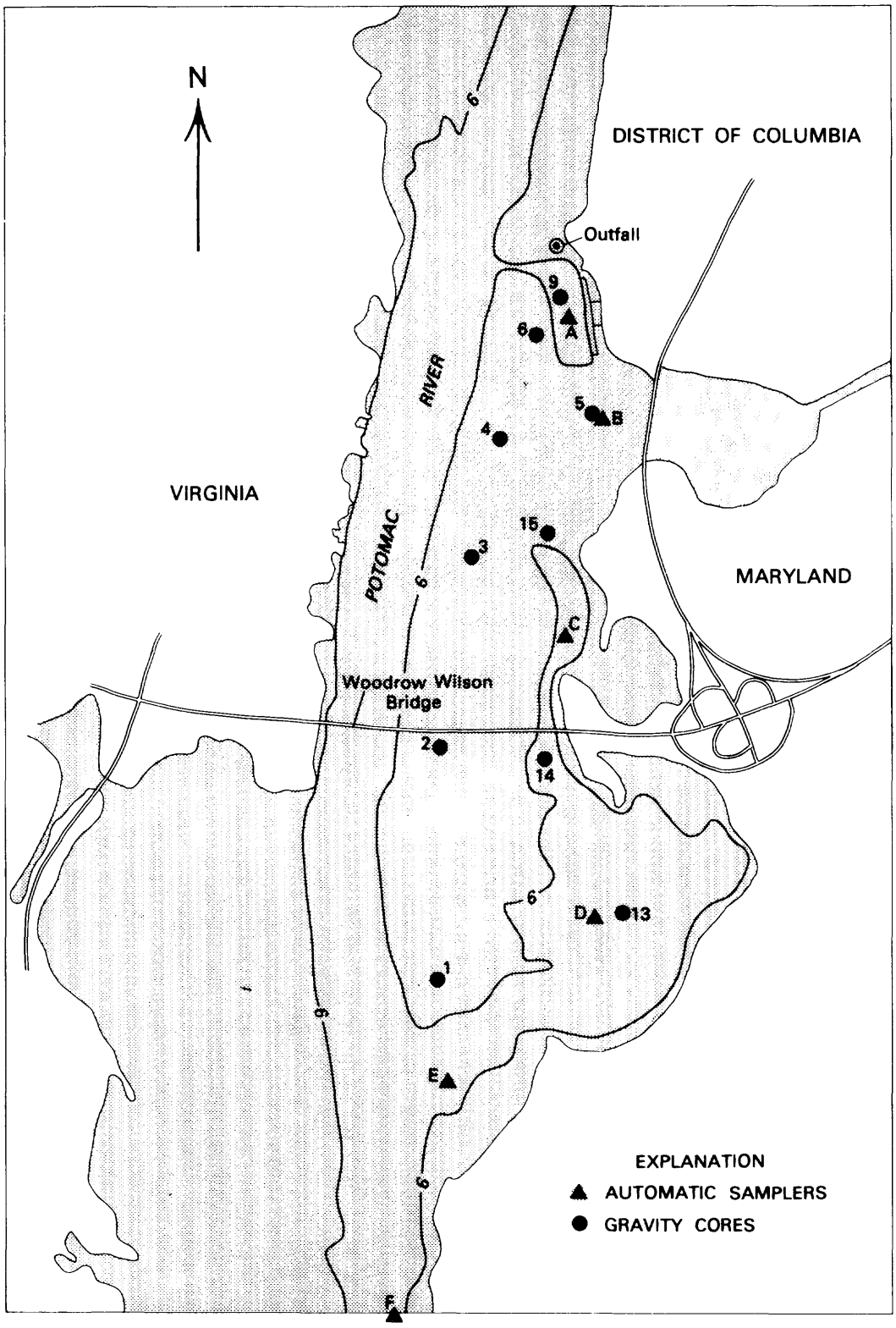

Figure 4. Automatic water sampler and gravity core stations for the August 1980 study. Six-foot depth contour indicates configuration of main channel and embayment.

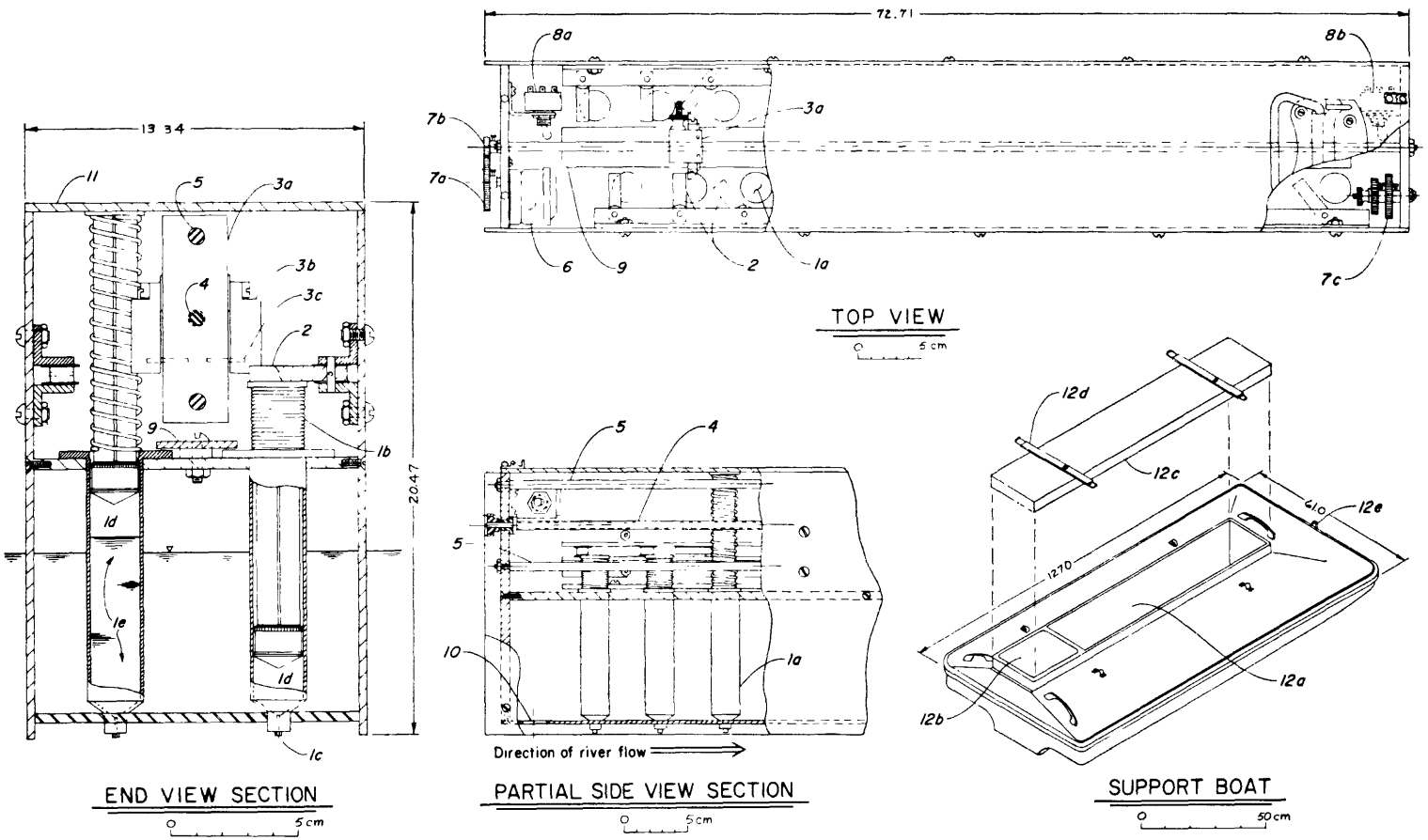

Figure 5. Automatic water sampler. From Kilpatrick (1972). 1*a*, 24 20-ml syringes; 1*b*, stainless steel compression spring; 1c, small-diameter opening preventing premature entrance of water; 1*d*, air pocket; 1e, water sample sucked in on release; 2, restraining bars; 3*a*, tripping block; 3*b*, trippers; 3c, restraining pins; 4, drive shaft; 5, guide and support rods; 6, dc timing motor, 7*a*, motor gear; 7*b*, shaft gear, 7c gear storage; 8*a*, off switch; 8*b*, reversal switch; 9, syringe retaining strip, 10, drain holes; 11, cover; 12*a*, open sampler well; 12*b*, sealed battery well; 12c, watertight cover, 12*d*, retaining straps; 12e, anchor bolt.

pole, depending on on water depth. Cellulose acetate butyrate coreliners, 7.7 cm in diameter, were used throughout the study. After collection, cores were immediately capped and transported to the laboratory at the Alexandria Coast Guard station.

Cores intended for solids analysis only were sampled by fitting a piston to the base of the core liner and removing samples as the core was extruded from the liner. Cores selected for pore-water analysis were sampled in a glove box purged with nitrogen. A piston was inserted into the bottom of the core liner, and hydraulic pressure was applied to force the core slowly from the liner into the glove box, where 2-cm sections were taken at the desired intervals.

Analytical Techniques

Dissolved phosphorus in water-column samples from both the September 1979 and the August 1980 studies was determined colorimetrically by the method described by Murphy and Riley (1962). Phosphorus determined by this technique is normally referred to as dissolved reactive phosphate, in that it represents only orthophosphate or forms of phosphorus easily hydrolyzable to orthophosphate by the sulfuric acid used. Dissolved chloride was determined colorimetrically by the mercuric thiocyanate method (Bergman and Savik, 1957).

Measurements of pH and Eh (oxidation potential) in the sediment pore waters were made inside the glove box by direct insertion of electrodes into each interval of sediment. After the electrode measurements were made, sediment sections were placed in nylon squeezers modeled after those described by Reeburgh (1967), and the pore water extracted by pressure filtration through 0.20-μm pore size membrane filters. After pore-water extraction, sediment cakes were stored in polyethylene jars and frozen until analysis.

The percent sand present, defined as the weight percent of the sample greater than 62 m in diameter, was determined gravimetrically after separation of the sand fraction by wet sieving. The grain-size distribution of the silt plus clay fractions of samples was determined by Coulter counter analysis.

Dissolved reactive phosphorus in the pore waters was determined colorimetrically by the technique used for the water-column samples. Iron and the four major cations present in the pore waters (Mg^{2+}, K^{+}, Na^{+}, and Ca^{2+}) were determined by flame atomic absorption using standard USGS techniques (Skougstad and others, 1979). Total solid phase phosphorus in sediments was determined by X-ray fluorescence (XRF), using a modification of the dilution-heavy-absorber technique described by Rose and others (1962). Ground samples were fused into pellets using a flux of $Li_2B_4O_7$ and were analyzed on a Diano model 8600 automated wavelength dispersive XRF spectrometer.

X-ray amorphous iron and aluminum in bottom sediments were determined by extraction with acid ammonium oxalate, using a method modified from the one described by Schwertmann (1964). This technique should selectively extract the noncrystalline phases of iron and aluminum without attacking crystalline oxides or silicates. Extractable iron, aluminum, and phosphorus were determined simultaneously in extract solutions by inductively coupled plasma emission spectrography.

Bulk mineralogy of bottom sediments was determined by X-ray diffraction using a Diano model XRD-5 X-ray diffractometer. Freeze-dried samples were ground, suspended in distilled water, pipetted onto glass slides, and allowed to dry at room temperature. Diffraction scans were made with Ni filtered, Cu K-alpha radiation at 50 milliampere and 40 kilovolt, using a scan rate of 1 degree per minute and a chart spacing of 1 inch per degree. The peak areas of designated reflections were measured using a planimeter. Results were expressed as percent diffracted intensity by dividing each peak area by the sum of all measured peak areas. This method should reflect relative differences between samples without the uncertainty associated with claims of quantitative measurement (Pierce, 1974). The characteristic d-spacings used to identify minerals are given in table 1.

Table 1. d-spacings used for the identification of minerals in bottom sediments
[A = Angstrom]

Mineral	hkl	Principal spacing (A) used for identification
Montmorillonite	(001)	15.0 (expands to 17 A after glycolation)
Illite	(001)	10.0 (broad reflection, with other basal spacings relatively small).[1]
Muscovite	—	10.0 (sharpness of reflection and intensity of 5.00 A reflection used to distinguish from illite).[1]
Kaolinite	(001)	Ratio of 3.54 A to 3.57 A peak applied to combined peak at 7.13–7.15 A.
Chlorite	(002)	Do.
Quartz	(101)	3.34.
Plagioclase	(002)	3.18.
Orthoclase	(220)	3.31.

[1]From Carroll, 1974.

Dye Injection and Analysis

Rhodamine WT fluorescent dye was chosen for both the September 1979 and the August 1980 studies. This dye has been shown to be superior to other commonly used dyes in terms of its stability and its susceptibility to complexation and adsorption (Smart and Laaldlaw, 1977). The dye was supplied by the manufacturer in a 20-percent solution of ethanol.

For the initial mapping of the effluent flow path during the September 1979 study, a single 45-kg slug of dye solution (9 kg of dry dye) was injected into the effluent from within the treatment plant.

For the determination of the residence time of the effluent during the August 1980 study, a continuous injection method was used. Two-hundred and twenty-five kilograms of dye solution (45 kg of dry dye) were injected into the effluent from within the treatment plant at a constant rate of 122 ml per minute for 1 tidal day (24.8 hours).

Dye concentrations were determined fluorometrically using a Turner model 10-0005R fluorometer. Preliminary calibrations were made using distilled water as well as filtered and unfiltered Potomac River water spiked with aliquots of dye. The results showed two possible sources of error. Spuriously high fluorometer readings were caused by the presence of particulate matter and by the presence of naturally fluorescing dissolved organic compounds in the river water samples. To avoid these interferences, all determinations were made on filtered samples, using standards made from filtered river water. A separate 1-cm path-length cell was used for each sample, so that the aliquot could be returned to the sample vial without the risk of dilution or contamination.

CIRCULATION REGIME AND PHOSPHORUS TRANSPORT IN THE STUDY AREA

Bathymetry

The bathymetric configuration of the study area has a marked effect on circulation in the vicinity of the Blue Plains treatment plant. The relative influences of river discharge, wind shear, and tides are all significantly affected by the bottom topography. A major feature in the study area is a shallow embayment on the eastern side of the river, which is separated from the main channel by a broad shoal area (see fig. 1). The embayment begins as an area of shallow flats near the treatment plant, narrows and deepens in the vicinity of the Woodrow Wilson Bridge, and finally widens out as it joins the main channel at a point approximately 4 km downriver from the outfall. Depths at mean low water vary from less than 1 m in the shallow flats to 5 m in the deepest part of the embayment. The only connection with the main channel at the upper end of the embayment is a narrow channel, which was dredged to allow access to the dock of the treatment plant.

The present configuration of the embayment resulted largely from the removal and addition of bottom sediments during various periods of dredging and dredge-spoil dumping during the past 100 years. Large quantities of sand and gravel were apparently dredged from the area during the early part of this century for use in building and in cement production (Fred Tilp, personal commun.). This dredging, which began as early as 1905 and continued into the 1920's, was primarily responsible for creation of the embayment. Additional isolation of the embayment from the main channel resulted from dumping of dredge spoil in the midriver shoal area, a practice that continued until the late 1960's. A chronological sequence of topographic maps (fig. 6) indicates how much the shoreline has been modified. The embayment does not appear on the 1879 map but was well developed by 1941. The larger of the two islands appearing on the 1941 map had disappeared completely by 1979, suggesting that the embayment was enlarged at least partially by natural erosion processes.

Influence of Bathymetry on Circulation

The effect of the bathymetric configuration of the embayment on the flow path of effluent from the treatment plant was first demonstrated by the dye study conducted in September 1979. Plots of dye concentration show the flow path of the tagged effluent (fig. 7). Following the injection at high slack tide, the dye patch moved rapidly downriver but was completely confined to the embayment. At low-slack tide the dye patch was centered in the lower portion of the embayment (fig. 7C), and with the ensuing flood tide it changed direction and moved back upriver. At no time during the sampling period was any dye detected above background levels at stations on the western side of the river or in the main channel. No dye was detected at the mouth of the small dredged channel, even though substantial concentrations of dye were still present near the outfall during flood tide. Quite clearly, the effluent flow path is confined to the eastern side of the river by the embayment, and under these flow conditions an effluent "parcel" takes more than one tidal cycle to travel from the outfall to the main channel.

The bathymetric configuration of the study area also has a marked effect on the response at different points to variations in river discharge. Figure 8 shows

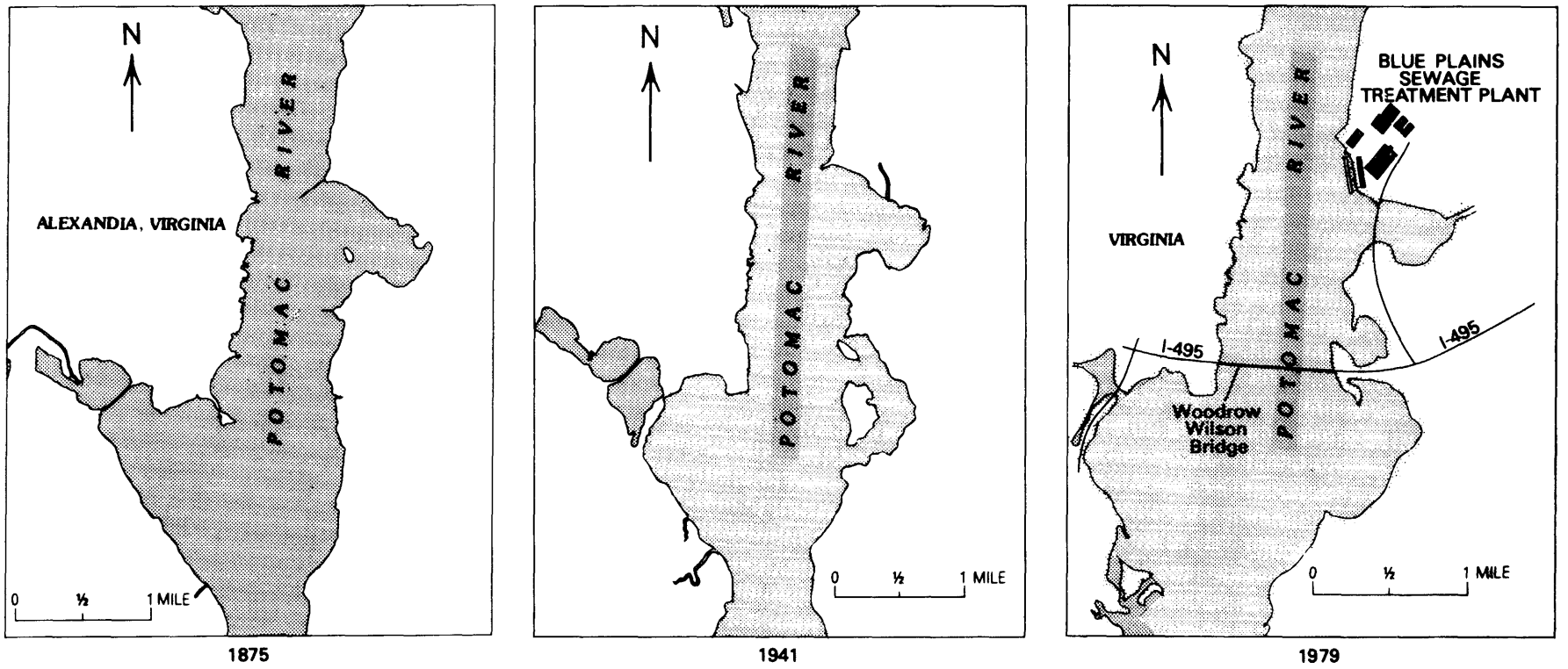

Figure 6. Physiographic evolution of the embayment on the eastern side of the Potomac River Source maps. 1975—U.S Coastal Survey Office, Potomac River Sheet No. 4; 1941—U.S. Geological Survey topographic map; 1979—U.S. Department of Commerce, National Ocean Survey Chart No. 12289.

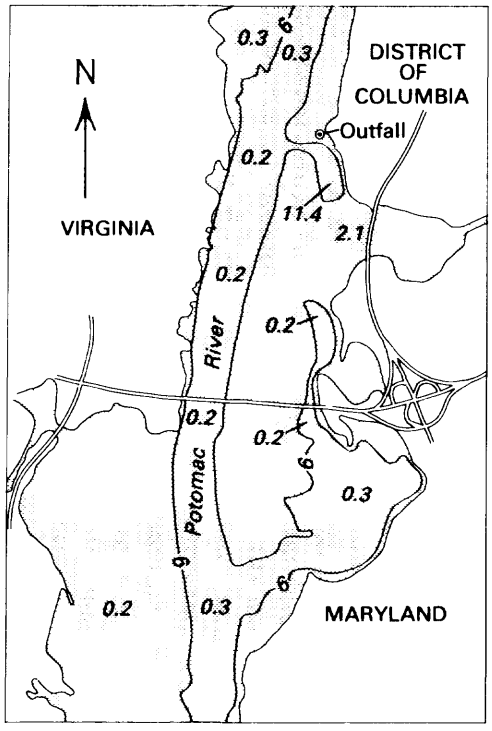

A. Two hours after injection

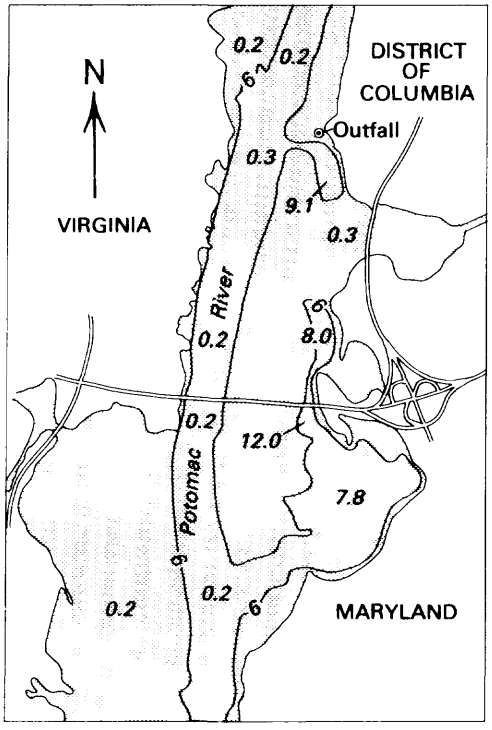

B. Five hours Maximum ebb

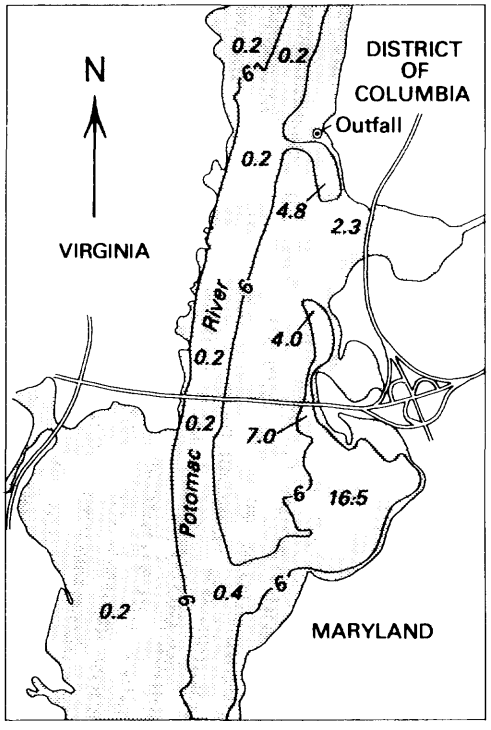

C. Eight and one half hours. Low slack

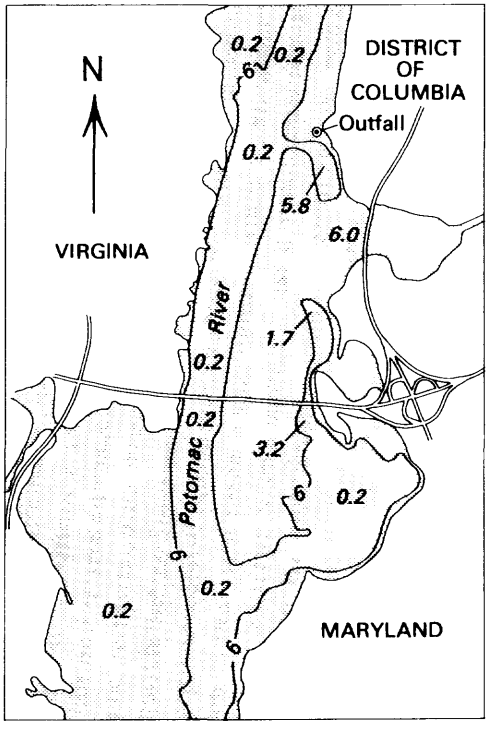

D. Eleven and one half hours. Maximum flood

Figure 7. Distribution of Rhodamine WT dye in the study area following the September 1979 slug injection. Dye concentrations reflect the confinement of the effluent flow within the embayment on the eastern side of the river. Numbers indicate ppb dry dye.

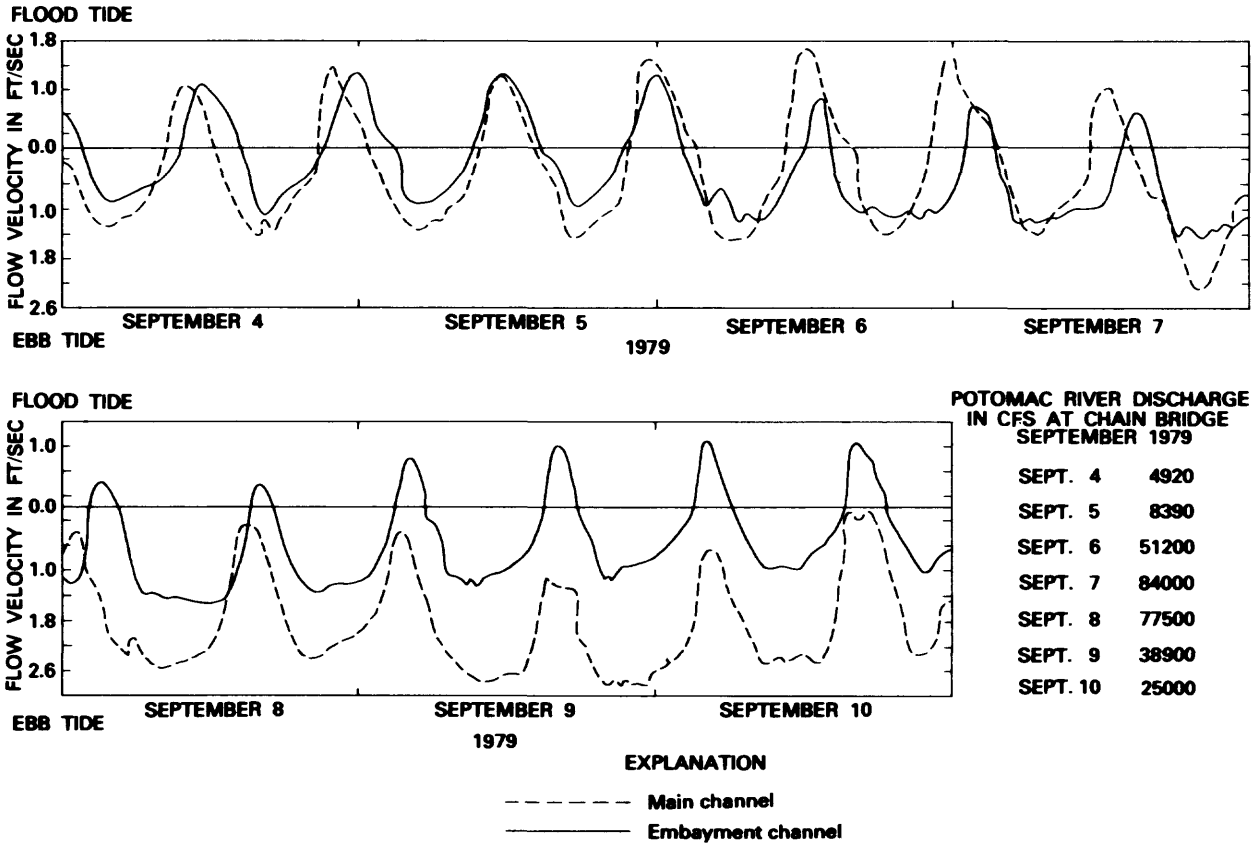

Figure 8. Flow velocity in the Potomac River near Wilson Bridge for the main channel and the embayment, showing the effects of Hurricane David, September 1979.

current meter records for the main channel and the embayment near Wilson Bridge during the period of high flow asociated with Hurricane David in September 1979 (Bob Baltzer, unpub. data). Prior to September 7, current velocities at both sites are comparable, the main channel downstream velocities being slightly higher. The moderately low flow is reflected by the proximity of ebb and flood-stage velocities. The effects of increased discharge are apparent beginning on September 7 and are markedly different at the two sites. In the main channel, ebb-stage velocities are more than doubled; upriver flow during flood stage is completely overwhelmed by the increased flow, and the flow direction is downriver throughout the tidal cycle. In the embayment, however, ebb-stage velocities show no significant increase; while velocities are substantially reduced during flood stage, the direction of flow is still upstream.

Clearly, the embayment is hydraulically separated from the main channel. Current velocities in the embayment appear to be primarily a function of tidal exchange; the effects of variations in river discharge appear to be limited to the main channel. If one considers the average current velocity for each area, the difference is probably even greater than is indicated by these data. While the point of measurement in the main channel is fairly representative of that stretch of the river, velocities in the embayment were measured at a point with one of the smallest cross-sectional areas. Velocities elsewhere in the embayment would be expected to be substantially lower.

The velocities shown in figure 8 probably represent the maximum values that would be expected in this area, with the exception of unusually high flow events. Records compiled by the Maryland Geological Survey show that average daily discharges in excess of 89,000 cfs (cubic feet per second) occurred only 0.5 percent of the time from 1930 to 1967; frequency of recurrence data show that 7-day flows in excess of 107,000 cfs occurred only once every 10 years.

Effect of Wind Shear on Circulation

The influence of wind shear on the movement of water within the embayment appears to be restricted to the shallow portion of the embayment near the treatment plant. Currents induced by wind shear in this area were particularly apparent during the August 1980 dye

study. During the early part of the sampling period, the wind blew from the south at velocities in excess of 20 miles per hour. The progress of the dye patch was slowed considerably, and small quantities of dye were observed moving northward past the outfall and toward the main channel. The southerly wind persisted for only a few hours, after which time the winds became northwesterly and the movement of dye toward the main channel was reversed. Although the quantity of dye released into the main channel near the outfall was minimal, it is apparent that persistent southerly winds of sufficient velocity could alter the flow path of the effluent. To evaluate the long-term effects of wind shear on effluent dispersion, daily wind direction and velocity data for nearby Washington National Airport for the period January 1976 to December 1979 were obtained from the National Weather Service. Wind rose diagrams were constructed of monthly average wind direction and velocity for each year (fig. 9). Easterly winds, which would be expected to cause significant movement of effluent into the main channel near the outfall, are highly unlikely. Southerly winds are somewhat more common, particularly in the summer and early fall. The dominant wind directions, however, appear to be from the southwest, west, and northeast. These winds would be expected to retard the movement of effluent into the main channel near the outfall. It would seem, therefore, that the flow path of the effluent usually should be confined to the embayment, as was indicated by the September 1979 dye study, and that the movement of effluent into the main channel near the outfall should be limited to relatively infrequent periods.

Effect of Circulation on Sediment Distribution

Although high-flow events such as Hurricane David are relatively infrequent, much greater quantities of sediment are transported during these periods than during the much longer intervals of low flow. One important result of the velocity differential between the embayment and the main channel is the marked difference in the grain size of bottom sediments in the two areas. Sediments in the main channel are predominantly sand size, while sediments in the embayment are largely silt and clay size (fig. 10). While fines are periodically scoured from the main channel during intervals of high flow, the protected nature of the embayment apparently facilitates the deposition of fine sediments. Substantial quantities of sand-size sediments in the embayment area occur only in the shallow area near the mouth of Oxon Creek (sites 5 and 6 on fig. 4). Sediments here are distinguished by a thin (10 cm) veneer of coarse sand which lies on top of finer sediments similar to those elsewhere in the embayment. Conversations with the Baltimore district of the U.S. Army Corps of Engineers confirmed that the coarse sediment is dredge spoil deposited during the late 1960's. Little if any deposition has occurred in this area since that time; fine sediments appear to have been winnowed away by wave action induced by wind shear.

Sediment distribution in the area around the treatment plant is particularly significant in terms of its effect on phosphorus transport. Phosphorus sorbed by suspended sediments will be more likely to be retained in areas of fine sediment accumulation; fine-grained bottom sediments will also continue to sorb phosphorus from the water column following deposition. On the other hand, the absence of fine sediments is believed to play a major role in the authigenesis of the phosphate mineral vivianite. Substantial quantities of this mineral have been found in the coarse sediments near the mouth of Oxon Creek. Specific mechanisms involved in the sorption of phosphorus by sediments and the precipitation of vivianite will be discussed in more detail in the section on geochemistry.

Mean Residence Time of Treatment-Plant Effluent

The length of time effluent remains in a given stretch of a river or estuary obviously limits the extent of its interaction with phytoplankton, suspended sediments, and bottom sediments in the area. For this reason, measurement of effluent residence time is a necessary complement to studies of geochemical or biological processes.

In a nontidal system, residence time is obtained by simply dividing the length of a given stretch of river by the average cross-sectional velocity. In a tidal system, however, the measurement of residence time is more complex because of the periodic reversal of flow direction. The concentration of effluent at any given point represents an accumulation of effluent parcels discharged over an interval of time. The total concentration of effluent will contain effluent that has just arrived at the point as well as effluent that passed the point at some previous time and then was transported back on a return flow cycle. Since measurements must take into account the presence of effluent parcels that left the source point at different times, residence time at a point must be expressed as an averaged value, or mean-residence time.

When one is attempting to determine the mean residence time of a solute being discharged into a body of water characterized by tidal flow patterns, it is often very difficult to employ the classical transport equations; these equations describe idealized conditions, and

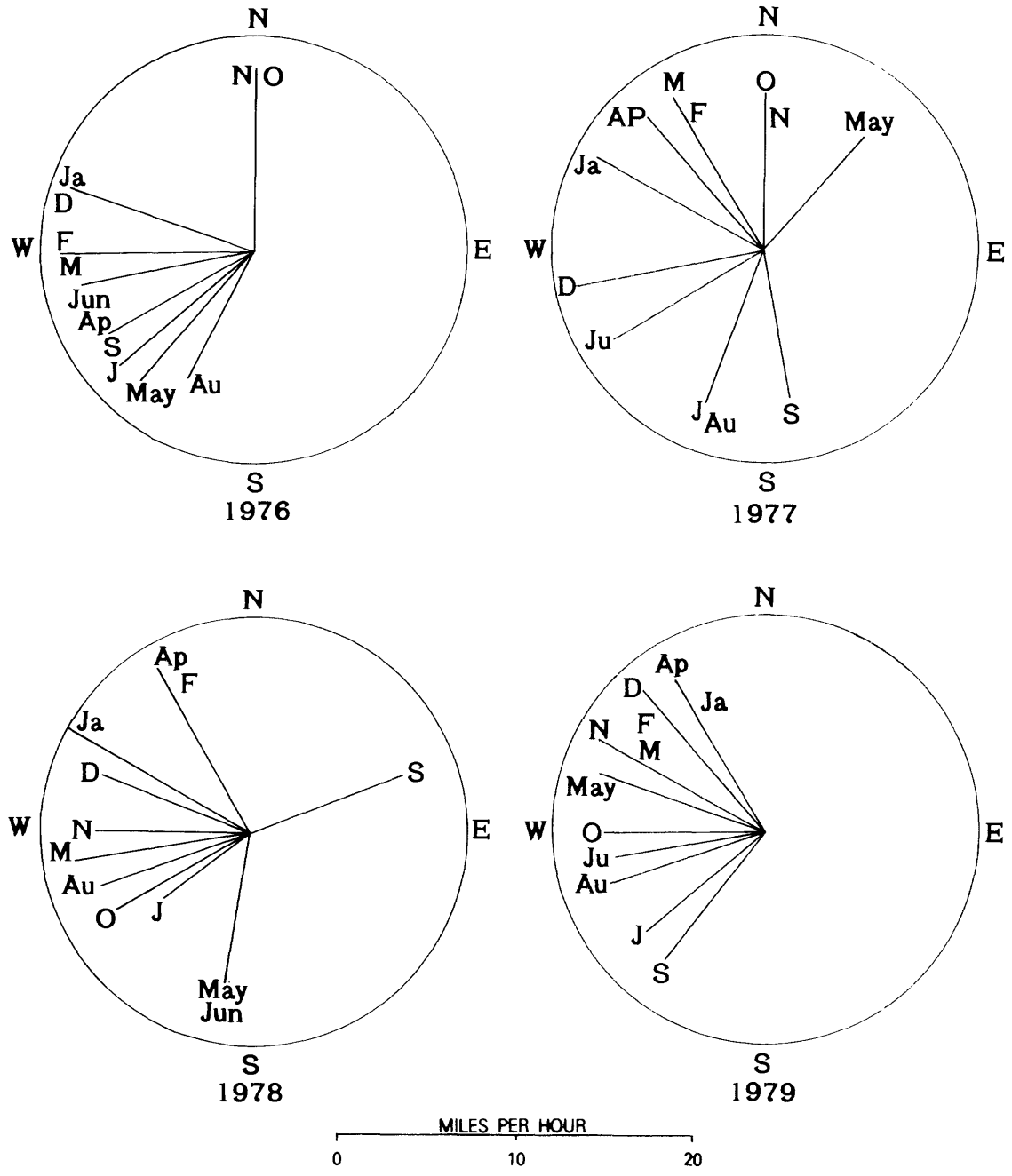

Figure 9. Average monthly wind direction and velocity at Washington National Airport for the period 1976-79.

flow parameters are usually poorly defined. However, if one makes the assumption that flow in the body of water is repetitive with a constant period, the mean residence time can be determined by dye injection using the method of linear superposition (Yotsukura and Kilpatrick, 1973), no matter how complex the flow patterns area. This technique is described in detail in appendix 1.

Forty-five kilograms of Rhodamine WT dye in 20-percent solution were injected at a uniform rate into an open conduit within the treatment plant for 1 tidal day (24.8 hours), beginning at 9:00 a. m. on August 11 and continuing until 9:40 a. m. on August 12, 1980. Surface-water samples were collected by the automatic samplers at 50-minute intervals during the first 80 hours of the test and at 120-minute intervals after this time until no dye was detected within the study area. Sampling ended on August 15, 1980. Time-response curves of dye concentration showed no dye at any of the stations after August 14 (fig. 11).

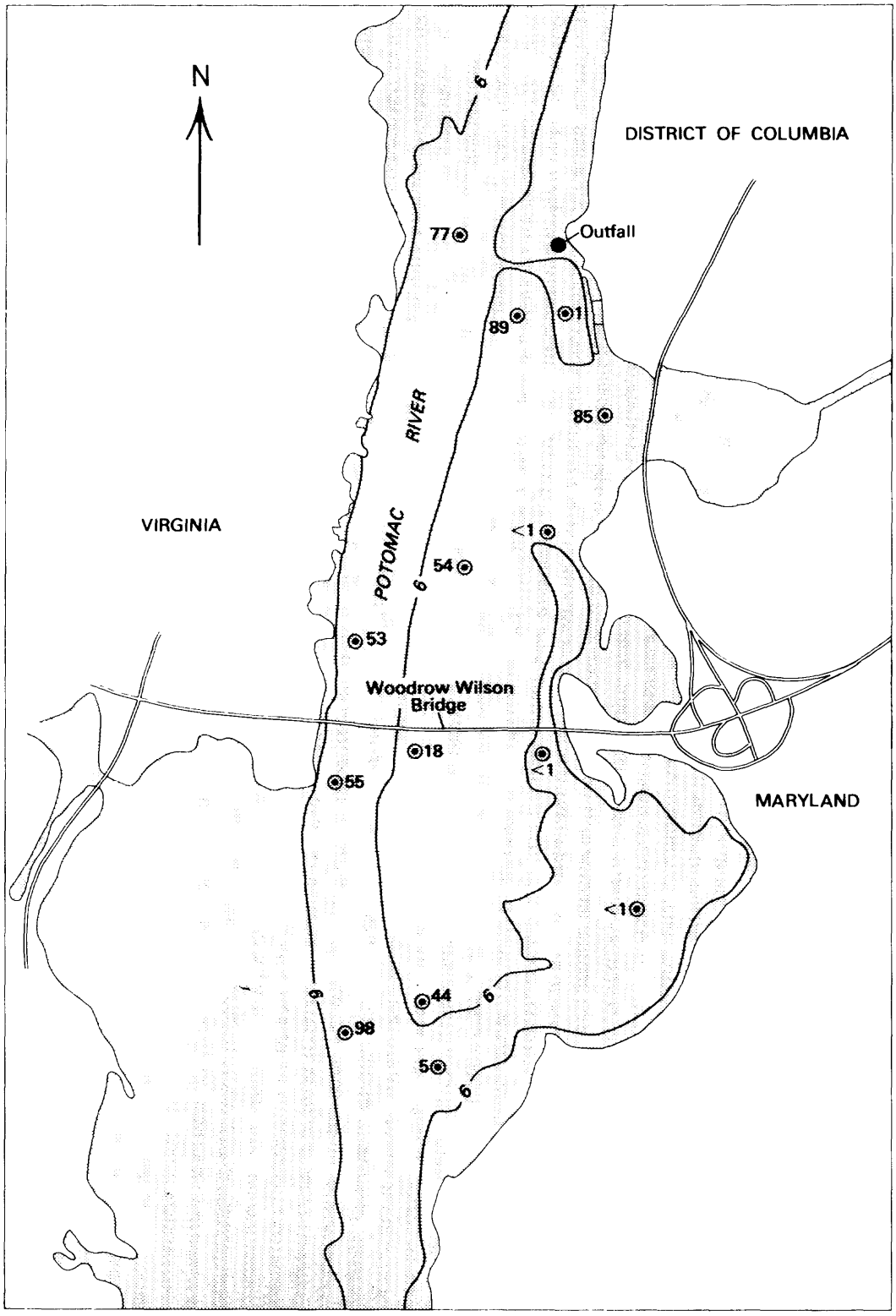

Figure 10. Weight percent sand in surficial sediments of the study area (Author's data plus unpublished data of Robert Cory and Jerry Glenn.) Six-foot depth contour indicates configuration of main channel and embayment

The mean-residence time for each sampling point was calculated using the equation derived in appendix 1 (fig 12). A period of 55 to 60 hours, or 2½ days, is indicated for the effluent to travel from the outfall to station F, (see fig. 4 for location of stations). As was mentioned earlier, the movement of dye close to the outfall was affected somewhat by southerly winds which persisted through the first half of the injection period. This is reflected in the anomalously high residence time for station B, where the progress of the dye mass was impeded by the effects of the opposing wind. As mentioned earlier, the effects of wind shear are also apparent in the lack of fine sediment in the area. In the deeper portions of the embayment, wind effects appear to be minimal. The current-meter data suggest that the residence time of the effluent in the embayment will not decrease substantially with increased flow; the data in figure 12 should therefore apply over a fairly large range of discharges. In contrast, if effluent were released in the main channel, its residence time would be expected to decrease markedly with increasing discharge.

GEOCHEMICAL AND MINERALOGICAL CONTROLS ON PHOSPHORUS MOBILITY

Adsorption of Phosphorus by Sediments

The capacity of soils to adsorb substantial quantities of phosphorus from solution has been known of for well over a hundred years. The first detailed description of the adsorptive quality of soils was published in

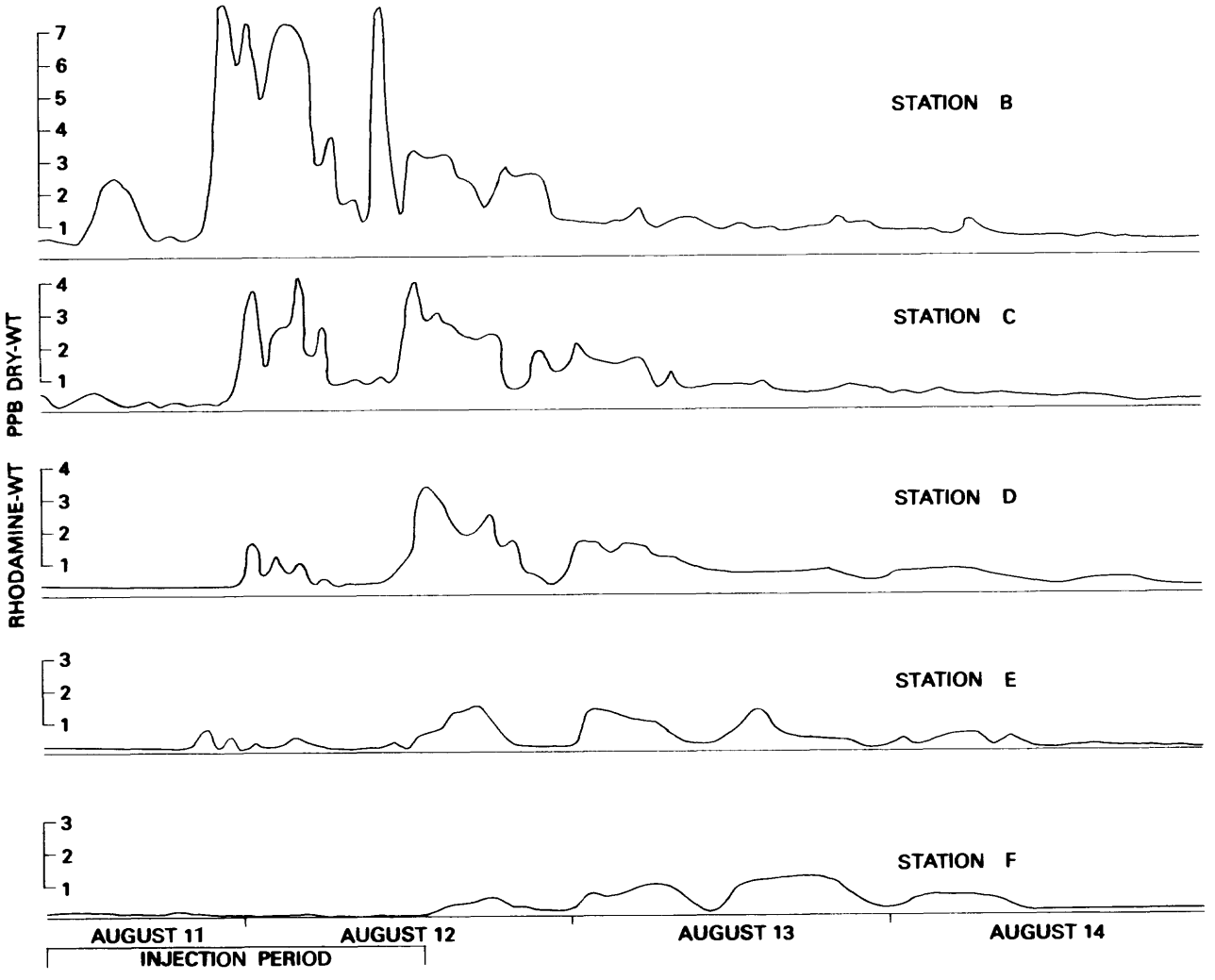

Figure 11. Time-response curves of dye concentration at stations B, C, D, E, and F

the "Journal of the Royal Agricultural Society" by J. T. Way in 1850. The adsorptive capacity of bottom sediments was recognized somewhat later; early studies by Einsele (1938) and by Mortimer (1941) showed adsorptive reactions with sediments to be a major control on the mobility of phosphorus in freshwater environments. The adsorptive properties of solid particles in natural waters have been attributed to the action of clay minerals, gels of ferric hydroxide and silicic acid, humus colloids, and living and dead organic matter. More recent studies of both soils and sediments have focused on the roles of clay minerals and the oxides of aluminum and iron.

Role of Iron in Phosphorus Adsorption

The adsorptive capacity of the oxides and hydroxides of iron was reported for soils as early as 1919 by Jennings, and for freshwater sediments as early as 1938 by Einsele. Phosphate adsorption capacity was found to correlate highly with the content of amorphous iron and alumina in a number of subsequent studies (McCallister and Logan, 1978; Saunders, 1964; Williams and others, 1971).

The mechanism of phosphorus adsorption of ferric oxy-hydroxides has most commonly been represented as a reaction with surface hydroxyl groups, some of which may be protonated (Parfitt and others, 1975):

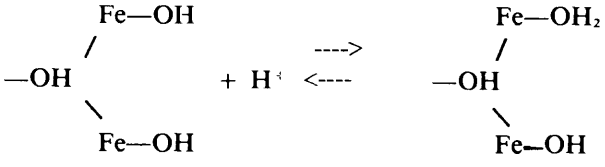

Ryden and others (1977), on the basis of Langmuir adsorption isotherms, suggested three separate and sequential mechanisms for phosphorus adsorption on iron oxide gels and soils. The first stage involves chemisorption by adsorption at a protonated hydroxyl site:

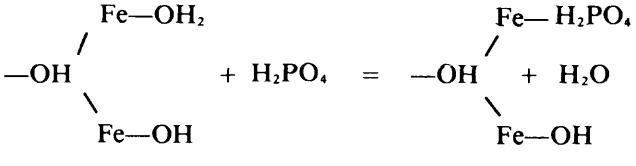

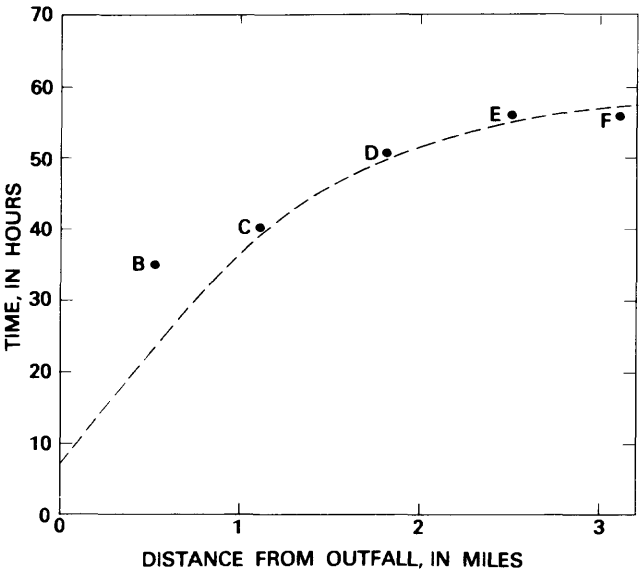

Figure 12. Mean effluent residence time as a function of distance from the outfall for stations B, C, D, E, and F.

The second stage involves chemisorption by the replacement of surface hydroxyl groups:

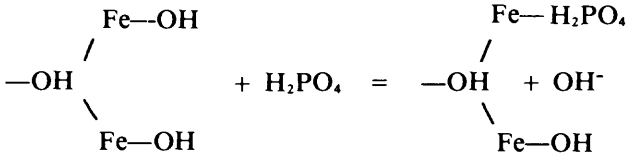

The final stage entails adsorption by weak physical bonding to surface ferric ions after chemisorption is complete. This model explains the commonly observed effect of pH on phosphorus adsorption. Decreasing pH will cause an increase in protonated hydroxyl groups and a corresponding increase in stage 1 phosphorus adsorption. The data of Ryden and others (1977) suggest that this model is applicable even up to pH 9, despite the fact that the phosphate species in solution changes from $H_2PO_4^{2-}$ to HPO_4^- above pH 7.2.

Role of Aluminum in Phosphorus Adsorption

The adsorption of phosphorus by aluminum in the form of silicates, hydrous oxides, and oxides has been the subject of study for many years (see reviews by Hemwall, 1957a, Larsen, 1967, and Black, 1968). Recent work has added new information to this subject, but the specific mechanisms involved remain somewhat unclear. Adsorption reactions appear to be similar to those involving iron in terms of the role played by surface hydroxyl groups, but they are complicated by the

participation of aluminosilicates. The protonation of surface Al-hydroxyl groups has the same effect as was described for ferric oxy-hydroxides; at lower pH values, more protons are available to create positive charges, and adsorption is enhanced.

Experiments with synthetic gibbsite suggest that phosphorus reacts with edge $Al(OH)H_2O$ groups, but that AlOHAl groups on the (001) face are nonreactive at low phosphorus concentrations (Parfitt and others, 1975). Adsorption isotherms for aluminum-containing surfaces are often linear at higher phosphorus concentrations (Muljadi 1966), indicating that adsorption sites are not diminishing despite continued adsorption. This may mean that new sites are being created during the adsorption process. Parfitt (1977) suggested that new sites could be created in gibbsite and kaolinite by the disruption of (001) faces or the adsorption of a second phosphate layer on edge surfaces. These conclusions are supported by the work of Veith and Sposito (1977), who reported significant release of Si into solution during the adsorption of phosphorus by synthetic aluminosilicates. Veith and Sposito (1977) concluded that phosphorus is assimilated by the secondary precipitation of Al-phosphates rather than through the formation of a surface O-phosphate phase by adsorption.

Role of Clay Minerals in Phosphorus Adsorption

Studies of phosphorus adsorption by the mineral components of sediments and soils have been confined largely to the layer silicates or clays. Numerous studies have shown that the clay minerals commonly present in soils and sediments vary considerbly in their ability to adsorb phosphorus. Edzwald and others (1976), using standard American Petroleum Institute clays, found the phosphorus adsorption capacity to increase in the order kaolinite < montmorillonite < illite. Lake and MacIntyre (1977) reported results showing adsorption capacity to increase in the order montmorillonite < kaolinite < illite < chlorite. The effect of pH on adsorption is similar to that observed in studies of iron and aluminum oxides: adsorption generally increases with decreasing pH.

Phosphorus adsorption by clay minerals has been attributed to reactions with hydroxyl groups on grain surfaces, to negatively charged edge sites on kaolinite, and to the surface precipitation of phosphate by free Fe, Al, and Ca. The intimate association of both amorphous iron and aluminum with many clays makes the evaluation of sorption effects exclusive to clay minerals quite difficult. The results of a number of studies suggest that amorphous iron phases may in fact be responsible for much of the variation observed between different mineral species. Both chlorite and illite may contain several weight percent of iron; the weathering of these minerals would be expected to produce surface coatings of amorphous iron. Phosphorus adsorption by illite has been shown to increase steadily as the pH decreases, reaching a maximum around pH 5 and then decreasing rapidly (Edzwald and others, 1976). This behavior is consistent with adsorption by amorphous iron phases; as more hydroxyl groups are protonated with decreasing pH, adsorption would be expected to increase. The pH at which adsorption begins to decrease is very close to the limit of stability for amorphous ferric-iron compounds; as the pH falls below this point, amorphous ferric-iron will be progressively converted to the ferrous form and solubilized (Garrels and Christ, 1965).

Relative Importance of Iron, Aluminum, and Clay Minerals in Phosphorus Adsorption

Although it is generally acknowledged that the oxides of both iron and aluminum participate in adsorption reactions with phosphorus, efforts to evaluate the relative importance of these phases have not been completely successful. While the role of aluminum is believed to be paramount by some workers (Hemwall, 1957b), substantial evidence indicates that iron is more important (Krom and Berner, 1980). There does appear to be general agreement that the type of phosphorus fixation is related to the adsorption capacity, whereby aluminum is the primary adsorbing agent in soils having low sorption capacities and adsorption by iron phases is predominant in soils having high adsorption capacities (Laverty and Mclean, 1961; Volk and Mclean, 1963).

Data from various phosphorus adsorption studies are given in table 2. These data should be used for approximate comparisons only, as experimental conditions varied from study to study. Adsorption capacities are expressed in terms of the linear adsorption coefficient K^*, except for that of iron oxy-hydroxides, which is expressed as J, or micromoles of P adsorbed per gram of adsorbent. K^* has units of ml $\cdot$ gm^{-1} and is defined as C'/C, where C' = the ratio of the mass of P adsorbed to the mass of adsorbent and C = the P concentration in solution at equilibrium. The adsorption capacity of geothite is expressed in terms of both K^* and J.

Parfitt and others (1975) found the adsorption capacity of ferric oxy-hydroxide phases to be more than six times that of geothite, which is comparable in adsorption capacity to the hydrous aluminum oxides studied by Veith and Sposito (1977). Values of K^* for both of these phases are considerably higher than the value calculated for chlorite, the clay mineral with the highest observed adsorption capacity.

Table 2. Phosphate adsorption data for different substrates

[Adsorption capacity expressed in terms of the linear adsorption coefficient K*, or as C (micromoles P adsorbed gram of adsorbent)]

Substrate	K*	C	Reference
Ferric oxy-hydroxides	---	630[1]	Parfitt and others, 1975
Hydrous aluminum oxide	2,400[2]	---	Veith and Sposito, 1977
Goethite	3,000[3]	---	Hingston and others, 1974
	---	100[3]	Parfitt and others, 1975
Chlorite	621[2]	---	Lake and MacIntyre, 1977
Illite	250[3]	---	Edzwald and others, 1976
	209[2]	---	Lake and MacIntyre, 1977
Montmorillonite	100[3]	---	Edzwald and others, 1976
	34[2]	---	Lake and MacIntyre, 1977
Kaolinite	20[3]	---	Edzwald and others, 1976
	35[2]	---	Lake and MacIntyre, 1977
Soils	80[3]	---	Khalid and others, 1977
Lake sediments			
Calcareous	35[3]	---	Li and others, 1972
Noncalcareous	25–35[3]	---	Li and others, 1972
Estuarine sediment	3,750[3]	---	Jitts, 1959
Estuarine sediment	250[3]	---	Pomeroy and others, 1965
Potomac River sediments	250[2]	---	Piercey, 1982
Anoxic estuarine sediment	1[3]	---	Krom and Berner, 1980

[1]Data as reported in cited reference.

[2]As reported in Krom and Berner (1980).

[3]Calculated from data in cited reference by author.

Although the results cannot be applied directly to natural sytems, these data show a fairly clear relationship: the adsorption capacity of amorphous iron exceeds that of amorphous aluminum, which in turn exceeds that of clay minerals.

SEDIMENT GEOCHEMISTRY AND MINERALOGY

Total Phosphorous in Bottom Sediments

The results of total phosphorus analyses show the sediments closest to the outfall and within the embayment to be enriched in phosphorus to a depth of 15 to 20 cm (fig. 13). Sediments below this depth are consistently lower in total phosphorus. In contrast, the sediments in the midriver shoal area are uniformly depleted in phosphorus relative to the embayment sediments and show no surface enrichment.

Mineralogy of Bottom Sediments

The mineralogy of bottom sediments is dominated by quartz, muscovite, and a relatively constant suite of clay minerals (fig. 14). The clay minerals include lllite, kaolinite, and chlorite. Minor amounts of k-feldspar or plagioclase are also present in most samples. An accurate estimate of the relative proportions of illite and muscovite present was not attempted. However, the sharpness of the 10 A (001) reflection and the consistent presence of the (002) multiple on X-ray diffractograms suggest that muscovite is dominant (Carroll, 1970). This is supported by the visual identification of muscovite in all samples with a binocular microscope.

There are no apparent lateral or vertical trends in the mineralogy of sediments in the study area. With the exception of sites 5 and 6 (fig. 4), which are slightly enriched in quartz, lateral variations in sediment mineralogy are largely random. It is not generally possible to distinguish sediments in the embayment (sites 9, 13, 14, and 15) from those in the midriver shoal area (sites 1, 2, and 3) on the basis of their mineralogy. The marked difference in grain size between sediments from these two areas apparently reflects the relative proportions of silt and sand-size quartz rather than variations in clay content. Vertical changes in mineralogy also appear to be random; this is probably due to episodic variations in depositional patterns associated with changing discharge levels.

There is no evidence of a mineralogical control on the distribution of solid-phase phosphorus in sediments at sites 1, 3, 9, 13, 14, and 15; the phosphorus content of these sediments seems to be more a function of the

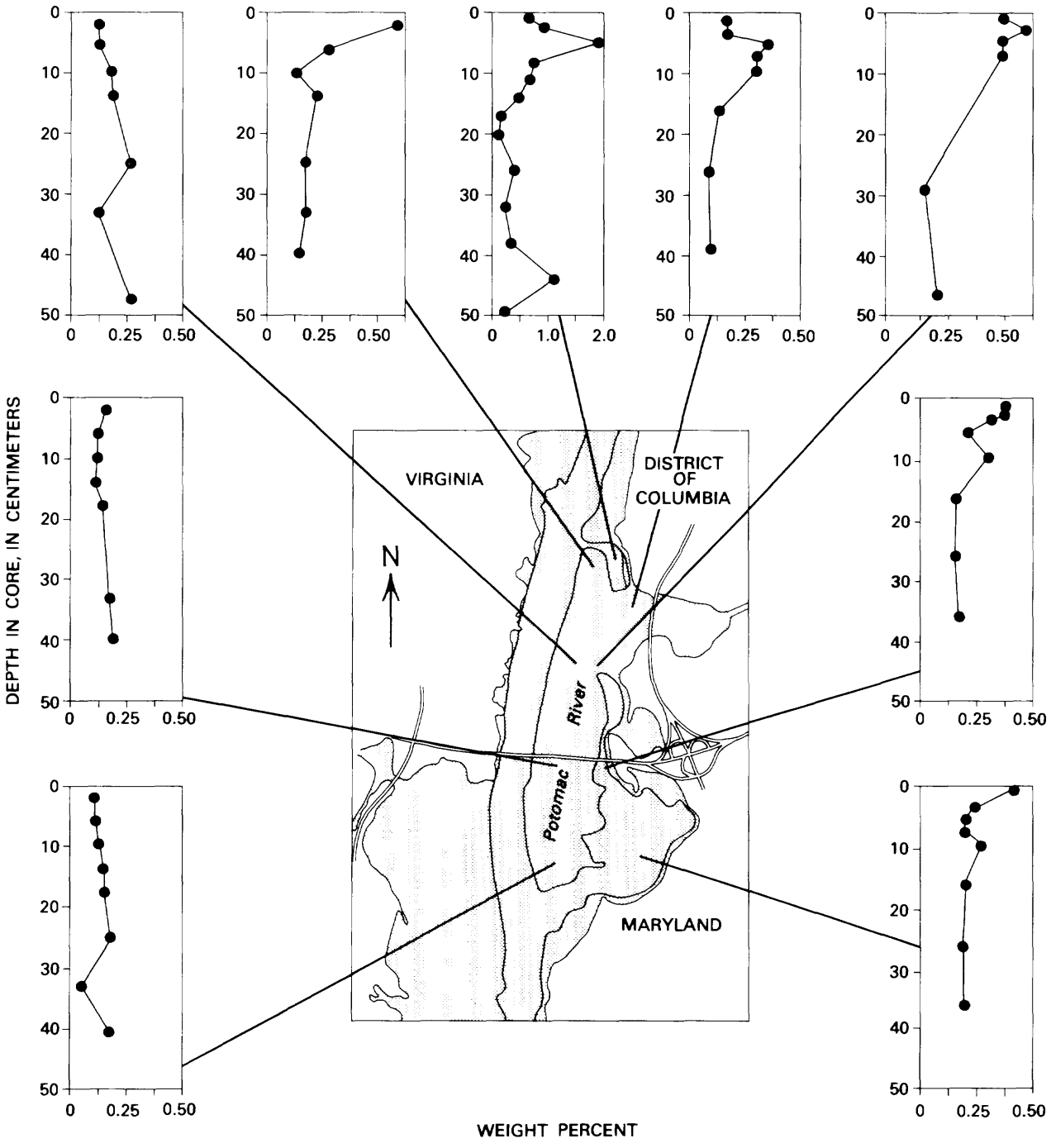

Figure 13. Vertical profiles of total phosphorus in sediments of the study area Values are expressed as weight percent elemental phosphorus in dry sediments

degree of exposure to the effluent than of mineralogy. The sediments at sites 5 and 6 may be exceptions; examination of samples from these locations by optical microscopy and by a scanning electron microscope equipped with an X-ray fluorescence analyzer (SEM/X-RF) revealed the presence of the ferrous-phosphate vivianite [$Fe_3(PO_4)_2 \cdot 8H_2O$]. The factors governing the occurrence of this mineral are discussed in detail below.

Oxalate-Extractable Iron, Aluminum, and Phosphorus in Sediments

The iron, aluminum, and phosphorus extracted by the acid-ammonium-oxalate technique should represent amorphous hydrated oxide and hydroxide phases only. However, because of uncertainty as to the absolute efficiency of the separation of amorphous from crystalline

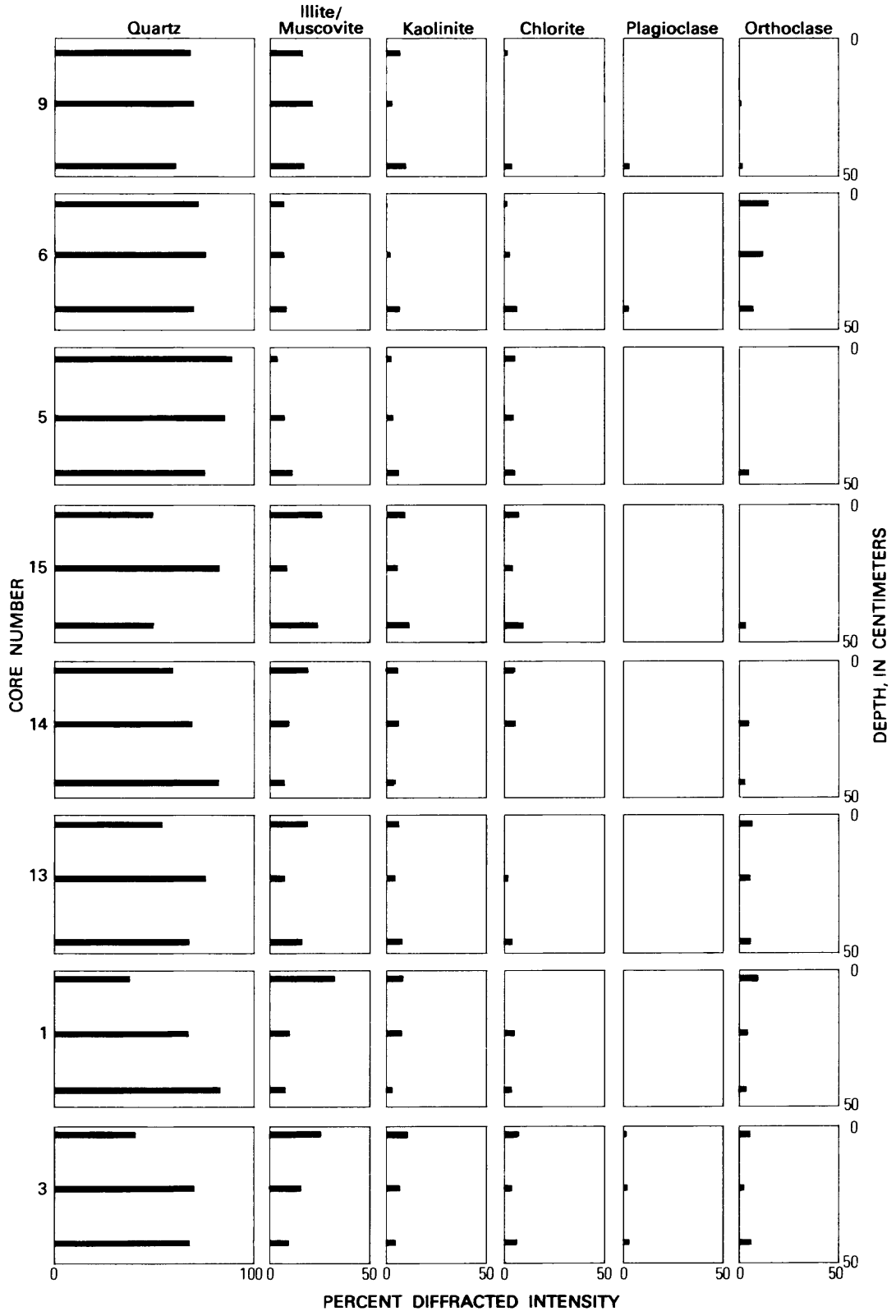

Figure 14. Bulk X-ray mineralogy of bottom sediments Values are expressed as relative percent diffracted intensity

phases, results are referred to as "oxalate-extractable" iron, aluminum, or phosphorus.

Profiles of oxalate-extractable iron, aluminum, and phosphorus show the highest concentrations of all three of these components at site 9, the site closest to the outfall (figs. 15–17). Extractable iron is present in core 9 in concentrations of up to 4 weight percent; concentrations in most other samples are on the order of 1 percent. Levels of oxalate-extractable aluminum and phosphorus are an order of magnitude less than those of extractable iron, with concentrations not exceeding 0.40 percent. With the exception of the coarse-grained sediments at sites 5 and 6, concentrations of extractable iron, aluminum, and phosphorus all diminish with in-

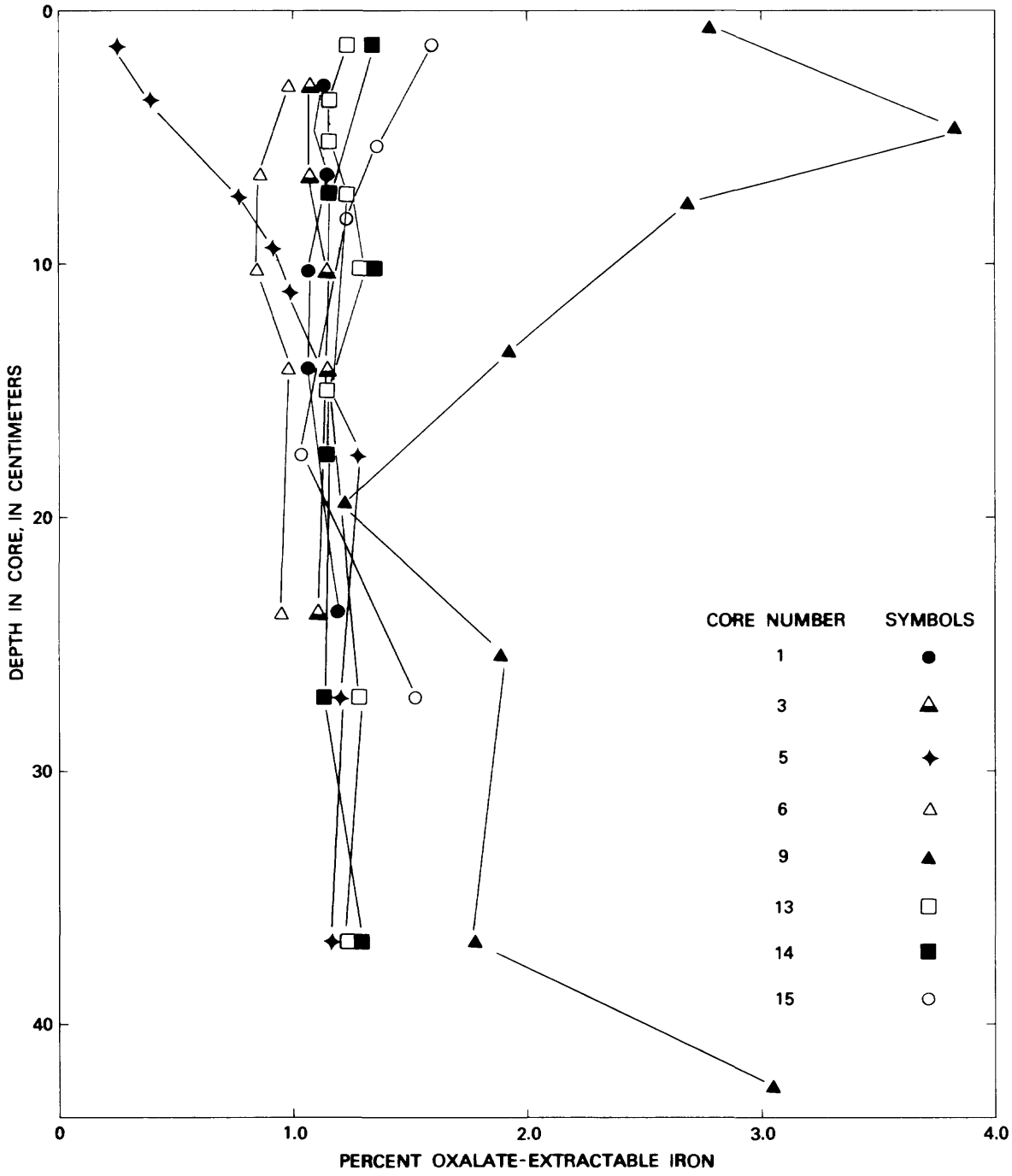

Figure 15. Vertical profiles of oxalate-extractable iron in bottom sediments.

creasing distance from the outfall. Surface sediments (above 10 cm) in the midriver shoal area contain lower concentrations of all three elements than do surface sediments in the embayment.

Total phosphorus shows a high degree of correlation ($r = 0.85$) with oxalate-extractable phosphorus (fig. 18). The high correlation of these data and the closeness of the regression line slope to 1 indicates that virtually all of the sediment-bound phosphorus is oxalate extractable. Cores 5 and 6, which contain substantial amounts of the ferrous phosphate vivianite in the surface layers, are an exception to this trend. Removing the data for these cores from the regression calculations improves the correlation from 0.85 to 0.99. While vivianite is

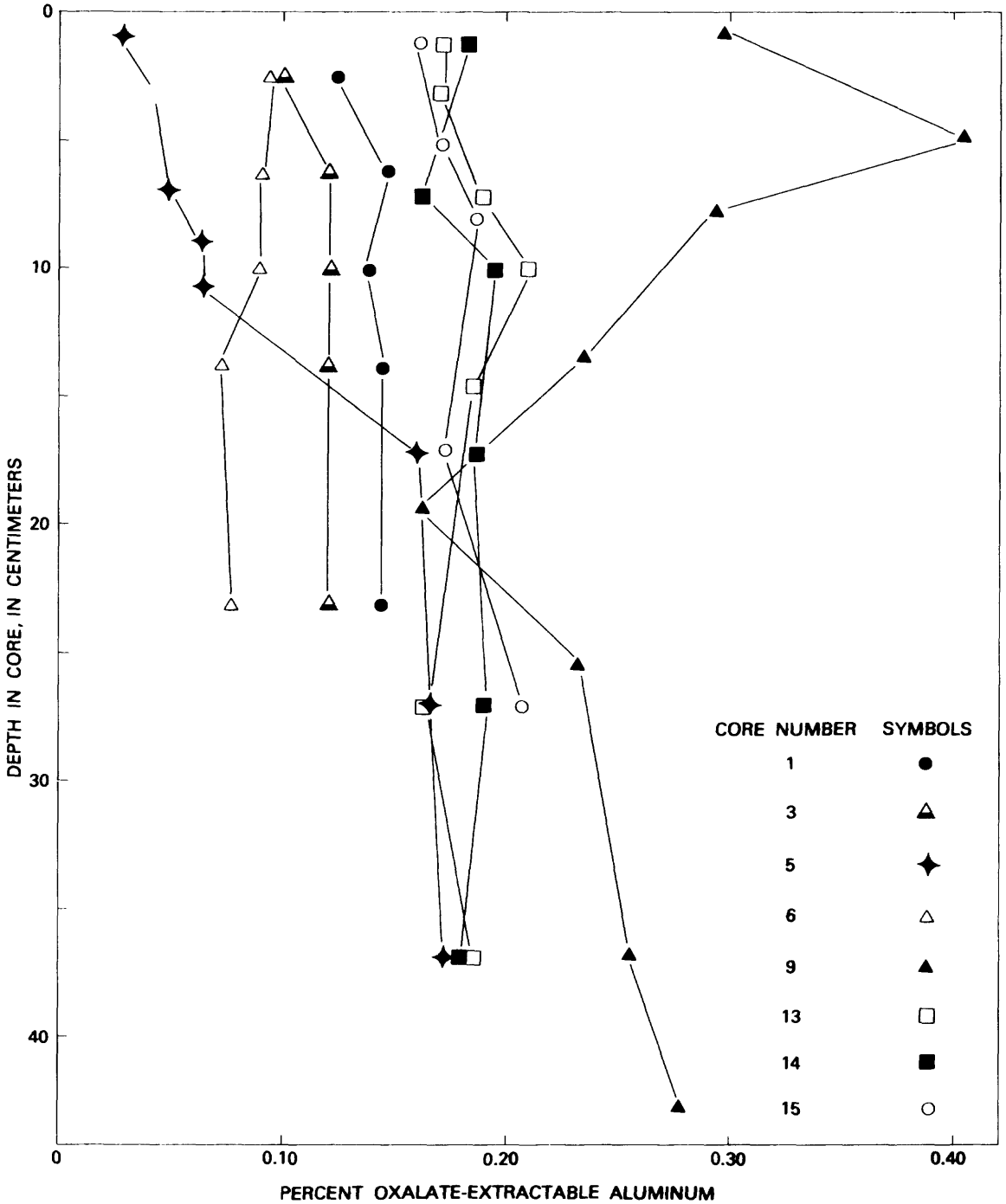

Figure 16. Vertical profiles of oxalate-extractable aluminum in bottom sediments

known to be attacked to a certain extent by oxalate extraction (Hearn and others, 1983), the data indicate that much less of the total phosphorus in these sediments was released.

Oxalate-extractable phosphorus correlates at a high level with oxalate-extractable iron ($r = 0.92$; fig. 19) and to a lesser degree with extractable aluminum ($r = 0.74$; fig. 20). While the correlation of extractable aluminum with extractable phosphorus is significant, the low concentrations of extractable aluminum relative to extractable iron suggest that it plays a much smaller role in the adsorption of phosphorus. Extractable iron is present in concentrations 6 to 14 times greater than extractable aluminum.

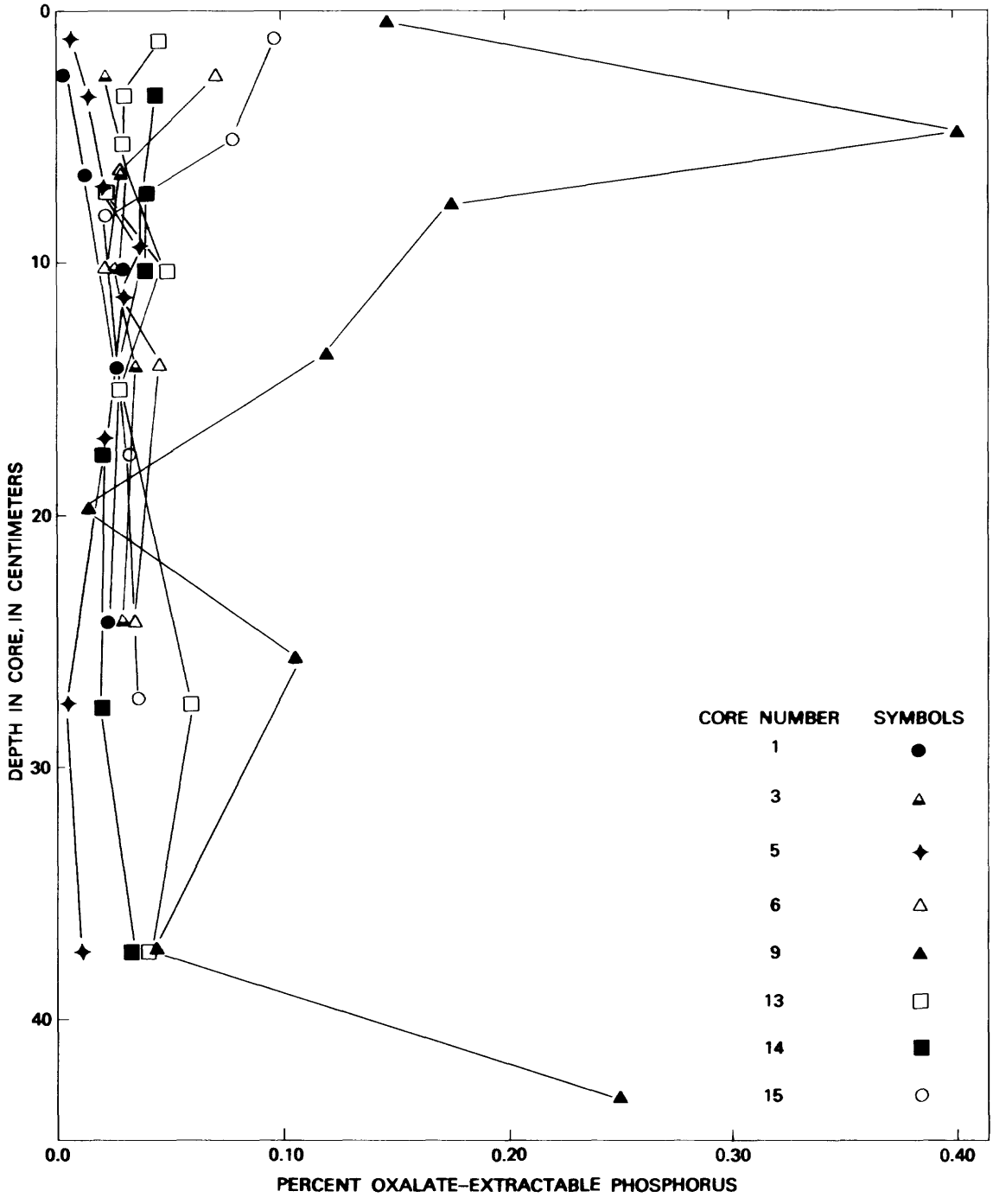

Figure 17. Vertical profiles of oxalate-extractable phosphorus in bottom sediments.

The importance of amorphous iron in phosphorus adsorption is also indicated by a comparison of the phosphate-adsorption capacity of sediments with their content of oxalate-extractable iron. Figure 21 shows a plot of phosphate-adsorption capacity calculated from Langmuir adsorption isotherms (data from Piercey, 1981) and the content of oxalate-extractable iron for sediments from various parts of the Potomac River and estuary. The high degree of correlation of these data suggests that amorphous ferric oxy-hydroxides are indeed playing a major role in the fixation of phosphorus by sediments.

Discharge of Particulate Iron and Aluminum by the Treatment Plant

The greater levels of oxalate-extractable iron and aluminum in the sediments closest to the outfall indicate that substantial amounts of amorphous iron and aluminum are being discharged with the effluent. With the exception of the coarse sediments at sites 5 and 6, concentrations of both elements diminish with increasing distance from the outfall within the embayment, and are lower still in shoal area sediments not exposed to the effluent.

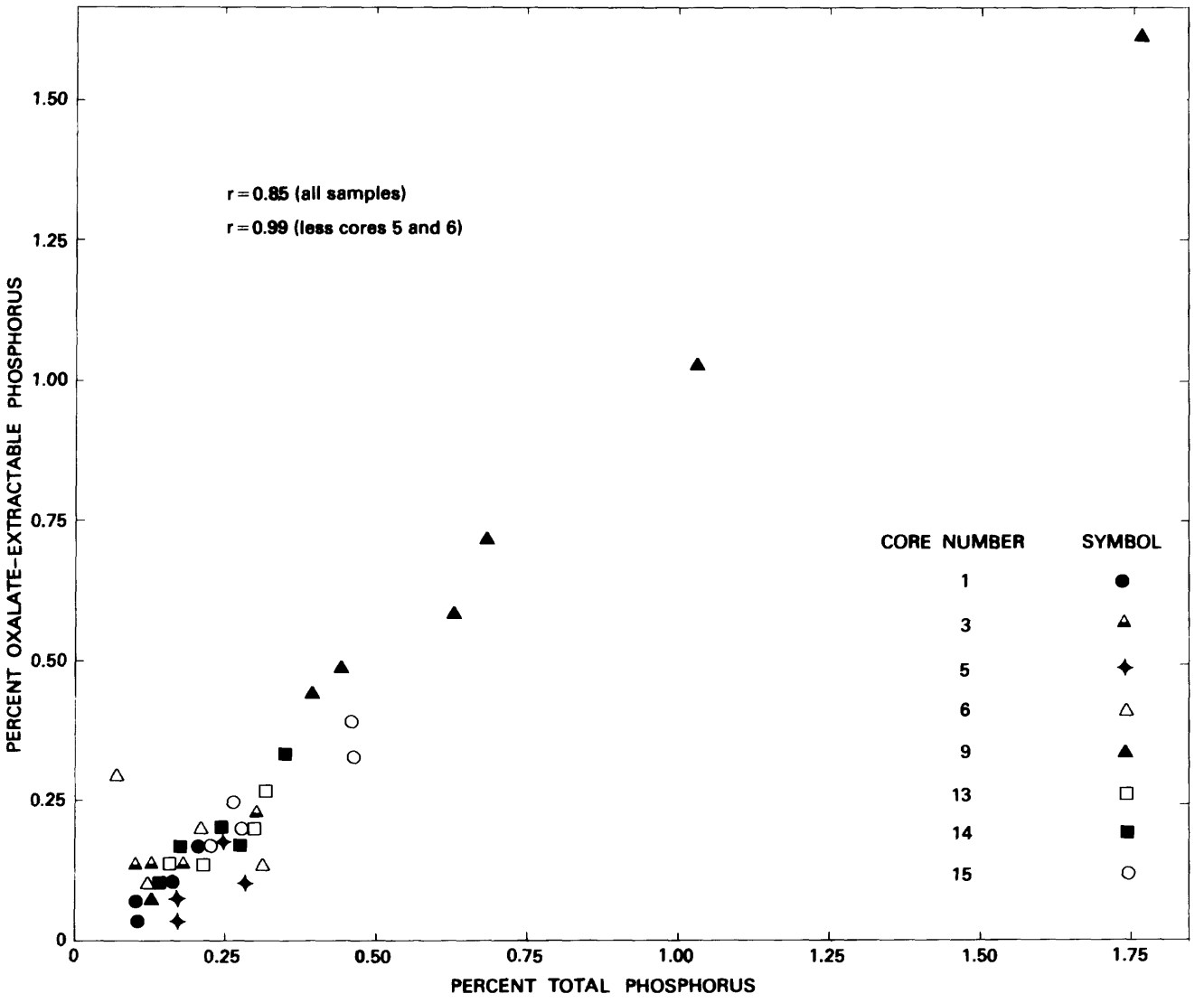

Figure 18. Oxalate-extractable phosphorus versus total phosphorus in bottom sediments.

The source of extractable iron and aluminum is most likely the combination of aluminum sulfate, ferric chloride, and ferrous sulfate which are added to remove dissolved phosphorus during the treatment process. Data on the aluminum content of particulate matter in the effluent are not available, but plant records indicate that the quantities of ferric chloride and ferrous sulfate used commonly exceed the amount of aluminum sulfate used by a factor of 10 or more. A former plant engineer has reported that the iron content of particulate matter in the effluent ranges from 10 to 15 percent by weight (Ed Jones, personal commun.). Despite the fact that the particulate content of the treatment-plant effluent has been reduced by a factor of 6 or more since 1977, when the present outfall was installed, a substantial amount of iron has been discharged during this period. Combining a conservative figure of 10 percent iron with records of discharge and particulate concentration yields a value of 5×10^6 kg of Fe discharged since 1977. While the greater part of this iron has probably been flushed out of the embayment, a considerable quantity has clearly been retained.

Degree of Phosphorus Saturation of Sediments

Virtually all of the phosphorus present in bottom sediments in the embayment area has been shown to be extractable with ammonium oxalate. The extraction data also suggest that amorphous iron phases are primarily responsible for phosphorus adsorption. If this is true, the ratio of oxalate-extractable iron to oxalate-extractable

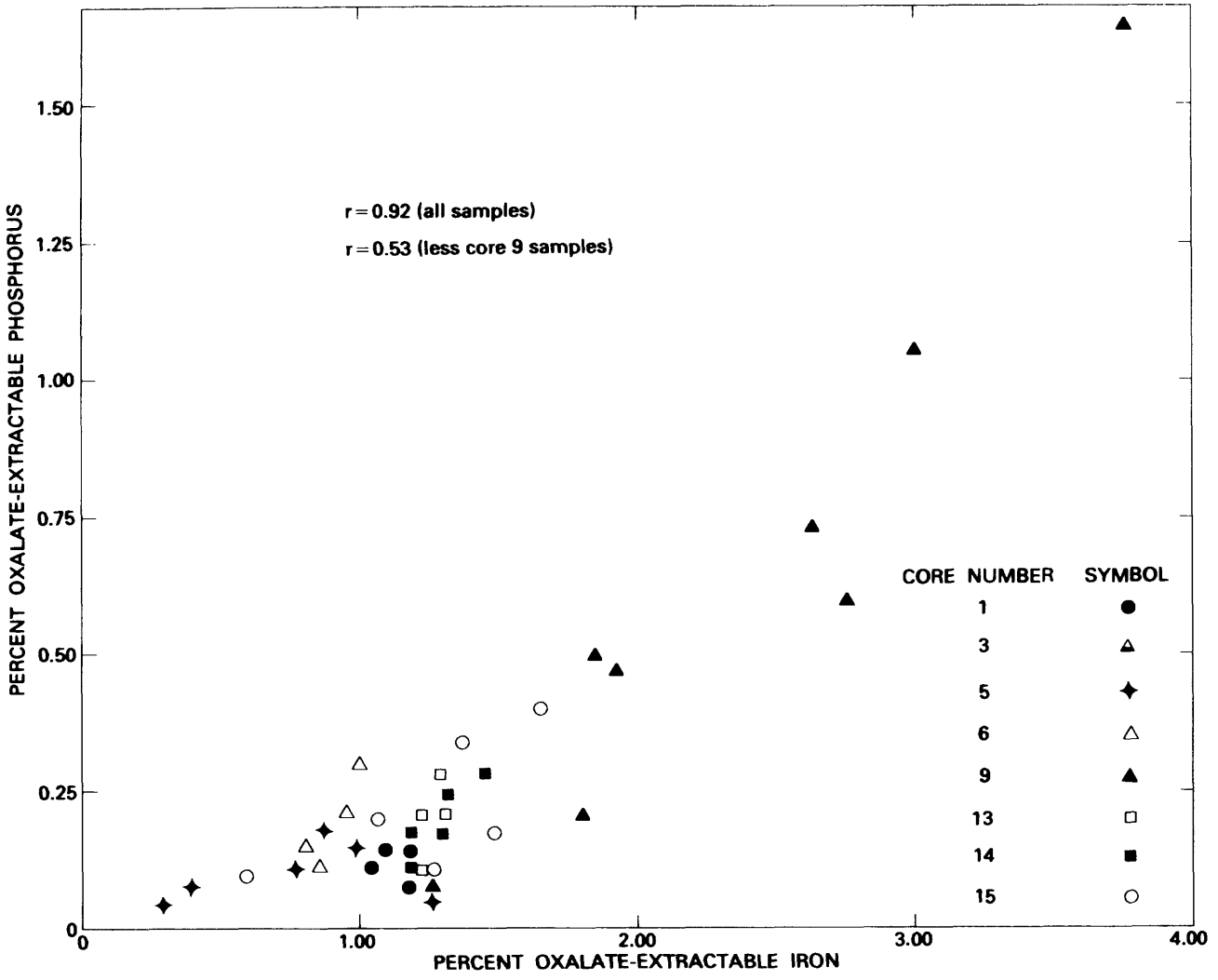

Figure 19. Oxalate-extractable phosphorus versus oxalate-extractable iron in bottom sediments.

phosphorus should provide a measure of the degree of saturation of bottom sediments in a given area. This ratio, which will be called the "phosphate-saturation ratio," should decrease steadily as more phosphorus is adsorbed and should approach a minimum value when all adsorption sites have been occupied. Average saturation ratios were calculated for the top 15 cm of cores within the study area. In figure 22, these values are plotted against the distance of the cores from the outfall, which should be a rough measure of the degree of exposure of the sediments to the effluent. Data from two other tidal river sites, 9 and 20 miles from the outfall, are also shown for comparison. As would be expected, sediments are decreasingly saturated with phosphorus with increasing distance from the outfall. The rate of decrease, however, appears to drop off sharply outside the embayment area. The saturation ratio increases steadily with distance from the outfall until site 1; the ratios from the two other tidal river cores are only moderately higher than these values.

Occurrence of Vivianite

Significant quantities of the ferrous phosphate mineral vivianite [$Fe_3(PO_4)_2 \cdot 8H_2O$] were found in the surface layer of dredge spoil in the shallow upper portion of the embayment. Most of the sediment-bound phosphorus not associated with amorphous iron and aluminum phases appears to be coor-

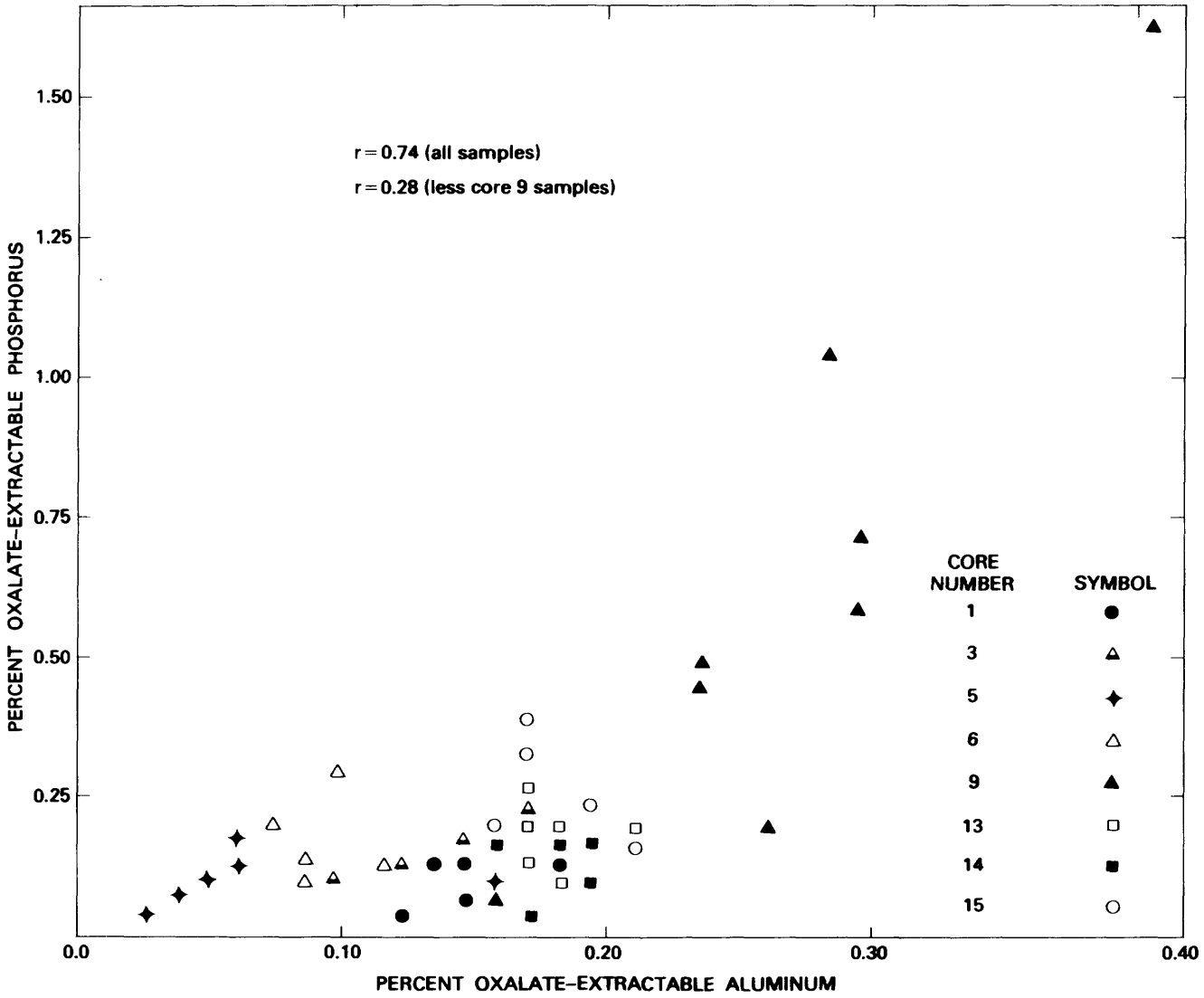

Figure 20. Oxalate-extractable phosphorus versus oxalate-extractable aluminum in bottom sediments.

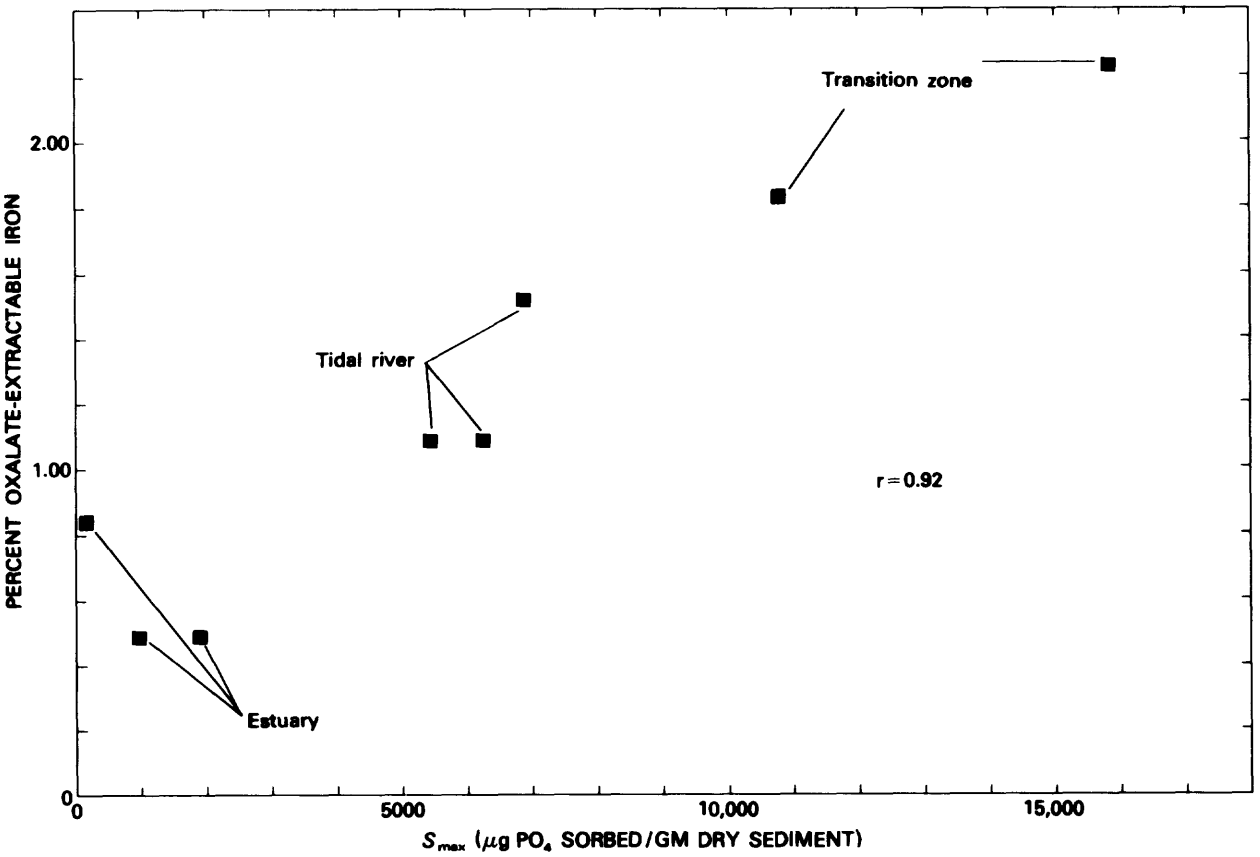

Figure 21. Plot of oxalate-extractable iron versus phosphate adsorption capacity (S_{max}) for surface sediments from various parts of the tidal Potomac River and estuary (after Piercey, 1981)

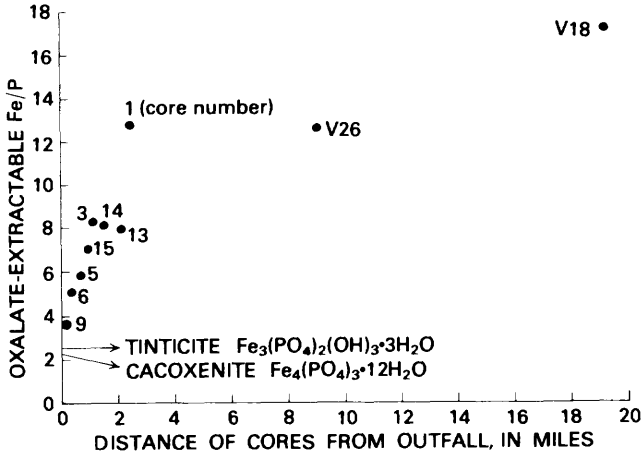

Figure 22. Phosphorus saturation ratio (oxalate-extractable iron/phosphorus) in surface sediments versus distance from the outfall. V18 and V26 are two other tidal river sites, 20 and 9 miles from the outfall, respectively.

dinated in this mineral. The greatest amounts of vivianite were found in the top 10 cm of cores 5 and 6 (see fig. 4). Substantially lower concentrations were found near the perimeter of the dredge-spoil area in the top 10 cm of core 15, where the surface layer is not predominantly coarse sediment. No vivianite was found below the 10-cm depth in cores 5, 15, or anywhere in any of the other cores.

The vivianite was initially identified by examination with an optical microscope and SEM/EDXRF. The particles found at site 5 are spherical aggregates of platy-, lath-, and needle-shaped crystals and are dark to light blue in color. The grain size ranges from silt to coarse sand, but most particles are between 200 and 300 μm in diameter. The particles found at site 15 differ from those found at site 5 in a number of respects. They are smaller (50 to 100 μm in diameter), are dark greenish blue as opposed to dark or light blue, and consist of more irregular aggregates of coarser platy- and lath-

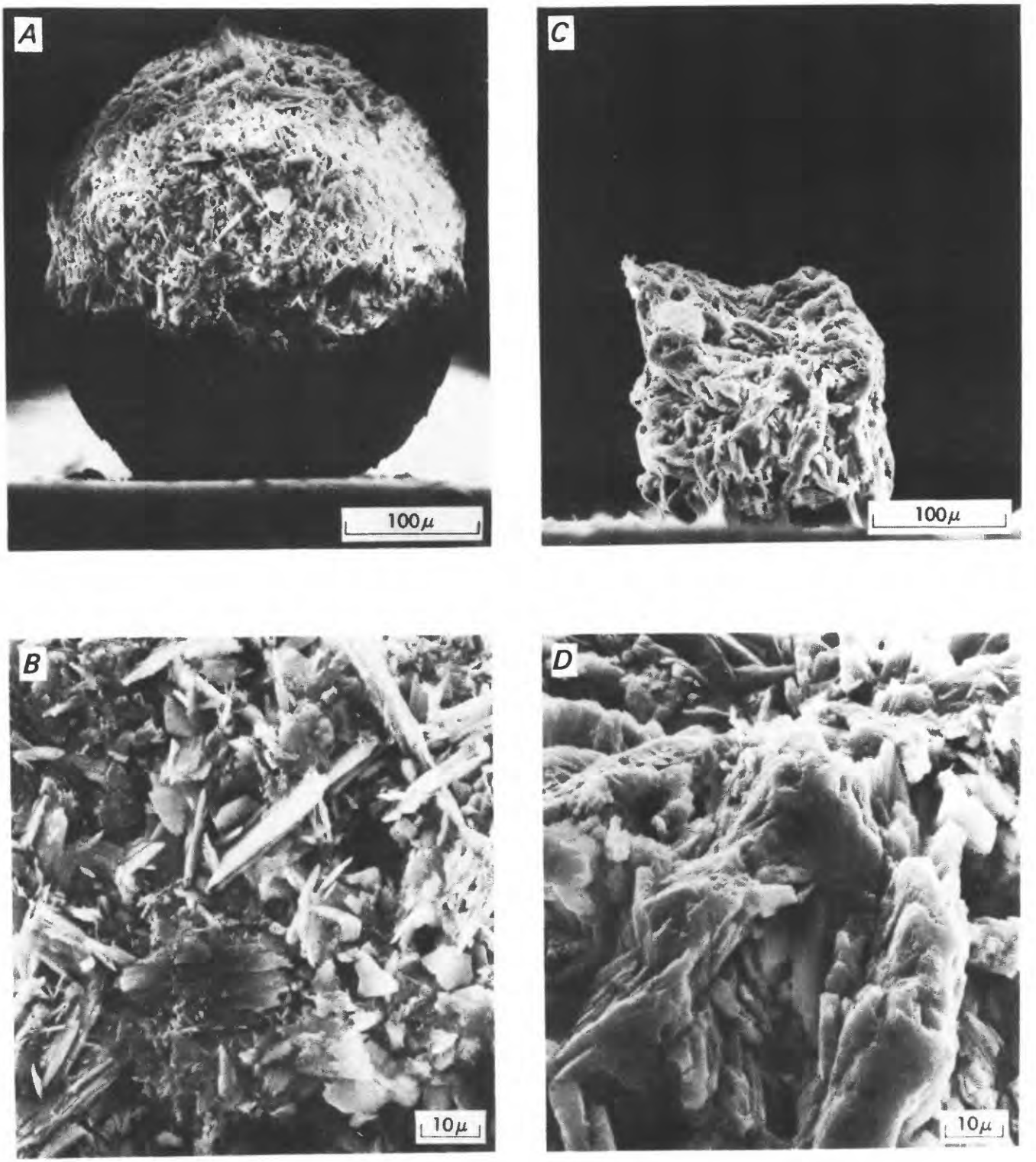

Figure 23. Scanning electron micrographs of vivianite crystals from cores 5 (*A* and *B*) and 15 (C and *D*).

shaped crystqals. Scanning electron micrographs of representative particles from each site are shown in figure 23.

The preliminary identification of vivianite from sites 5 and 15 was confirmed by X-ray diffraction analysis of single particles using a Debye-Scherrer powder camera. Diffraction patterns from each site were identical. No significant differences were found between the measured d-spacings and those reported for synthetic vivianite by Barth (1937).

Several factors indicate that the vivianite at site 5 is authigenic and was not introduced with the dredge spoil. The largest vivianite particles at this site are approximately 300μm in diameter, while the mean grain size of the sediment matrix is roughly 450 μm. Pure vivianite has a specific gravity of 2.68, close to what would be expected for the quartzose sediment matrix. If the vivianite particles were detrital, they should reflect the size distribution of the matrix in which they were transported. This is clearly not the case. Furthermore, with a hardness of 1.5 to 2, vivianite is quite vulnerabe to mechanical abrasion during transport. Particles at site 5 show no evidence of any such abrasion. The spherical shape of the particles and the euhedral nature of the individual crystals on particle surfaces also suggest that they have grown in situ.

In contrast to the particles found at sites 5 and 6, the vivianite from site 15 shows evidence of both mechanical and chemical alteration. Fresh vivianite is colorless but alters to blue and then to green with increasing exposure to oxygen (Dana, 1950). This color change is due to a partial oxidation of ferrous to ferric iron. The greenish-blue color of the vivianite particles from site 15, together with their irregular appearance and the absence of smaller euhedral crystals on aggregate surfaces, suggests that oxidation and mechanical abrasion have occurred during transport. These particles probably were formed closer to the center of the dredge-spoil patch and were subsequently reworked to the outer edge by the combined action of waves and tidal currents in the area.

Pore-Water Chemistry

To obtain more information regarding the formation and stability of the various phosphate phases present, the cores from sites 5, 13, 14, and 15 in the embayment area were selected for pore-water analysis. Plots of Eh, pH, dissolved iron, dissolved-reactive phosphate, and mean grain size are shown in figure 24.

Several factors distinguish the sediments at site 5 from the other three locations within the embayment. The differences are most apparent within the zone

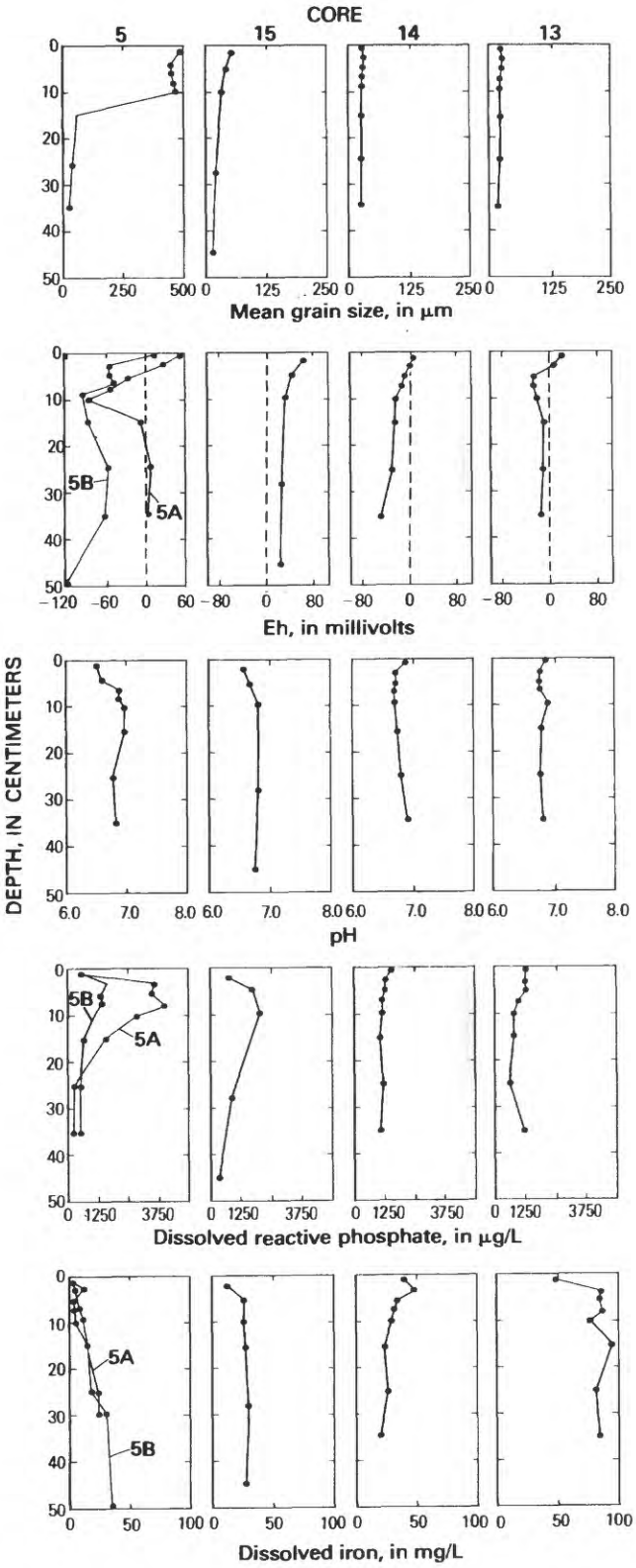

Figure 24. Vertical profiles of mean grain size, pore-water Eh, pH, dissolved-reactive phosphate and dissolved iron at stations 5, 15, 14, and 13.

where the vivianite was found. The layer of coarse dredge spoil in the top 10 cm of core 5 is obvious in the plot of mean grain size. A minor amount of coarse sediment is evident in the surface sediments at site 15, while sites 14 and 13 are characterized by uniformly fine silt and clay. The Eh profiles for site 5 are distinct, showing lower potentials in the zone of maximum vivianite concentration. Dissolved-reactive phosphate levels increase markedly within the coarse layer at site 5 and then drop in the underlying fine sediments. This trend is also present in core 15, but not in core 14 or 13. Dissolved-reactive phosphate levels in the coarse zone of core 5A are twice those observed in any other core. The dissolved-iron profiles at site 5 are also unique; concentrations increase regularly with depth, with iron levels in the surface zone lower than those at any of the other sites.

Significantly, dissolved-reactive phosphate values do not exhibit vertical gradients suggestive of upward diffusion from depths below 20 cm (see figs. 13 and 24); this trend is in agreement with pore-water data from other locations in the tidal Potomac (Callender, 1982). Thus the observed enrichment of total phosphorus in the upper 10–20 cm of the sediment column in the embayment cannot be explained by the remobilization and diffusion of dissolved phosphorus from underlying sediments. The most logical explanation is that the enrichment is due to the deposition of suspended sediment which has adsorbed phosphorus during contact with effluent. This model appears consistent with other evidence. When the cores for this study were collected, the outfall had been in use for approximately 3 years (September 1977 to August 1980). Although data for the embayment are not available, sedimentation rates as high as 6 cm per year have been estimated for nearby locations in the tidal Potomac by the ^{210}Pb technique (Ann Martin, unpub. data). Thus, the deposition of a 10- to 20-cm layer of sediment enriched in phosphorus by contact with effluent would appear quite possible.

Role of Ferric Oxy-hydroxides

Ferric oxy-hydroxides normally occur as colloidal gels, or coatings on mineral surfaces, and are usually concentrated in the fine size fractions of sediments (Carroll, 1958; James, 196; Jenne, 1977). Thus, one would expect to find less amorphous iron in the coarse sediments at sites 5 and 6 than in the silty-clayey sediments found elsewhere in the study area. The lower concentrations of amorphous iron observed at site 5 (see fig. 15) could explain the relatively high concentrations of phosphorus in the pore waters of these sediments, since adsorption by amorphous iron would be expected to prevent the accumulation of dissolved phosphate in sediment pore waters. And since the ferrous-ferric couple is one of the major controls on the platinum-electrode redox potential, the absence of ferric oxy-hydroxides could also account for the lower potentials observed.

Although the possible contribution of dissolved phosphorus and ferrous iron by the reductive dissolution of ferric oxy-hydroxides at site 5 cannot be completely discounted, this seems unlikely in light of the coarseness of the sediment. Analyses of oxidized coarse sediments elsewhere in the Potomac River have shown similar depletion in oxalate-extractable iron; it would seem that the absence of these compounds in sandy sediments is better explained by the winnowing of fines than by reductive dissolution. Although the accumulation of dissolved reactive phosphate at site 5 may be partly attributable to the dissolution of minor amounts of amorphous iron, the evidence suggests that dissolved phosphate derived from organic particles was concentrated in the pore waters at this site owing to the absence of phosphorus-scavenging ferric oxy-hydroxides.

Phosphate Mineral Equilibria

The low concentrations of dissolved-reactive phosphorus and the absence of fresh vivianite in cores 15, 14, and 13 suggest that phases other than vivianite are controlling the concentrations of phosphorus and iron at these sites. Several iron-phosphate minerals should be stable under conditions encountered in freshwater sediments. Nriagu and Dell (1974) have suggested that the ferric phosphates tinticite $[Fe_3(PO_4)_2(OH)_3 \cdot 3H_2O]$ and cacoxenite $[Fe_4(PO_4)_3 \cdot 12H_2O]$ should form under oxidizing conditions by the adsorption of phosphate ions onto ferric hydroxides. The disseminated nature of these phases, and the low concentrations that would be expected (probably less than 1 percent by weight), would make their detection by standard X-ray diffraction techniques very difficult. However, the presence of substantial concentrations of ferric oxy-hydroxides and dissolved phosphorus favors the formation of these compounds in the study area. The Fe/P ratios of tinticite and cacoxenite are 2.7 and 2.4, respectively. The ratios of oxalate-extractable Fe/P for sediments in the study area approach these values at site 9, where the phosphorus saturation is the greatest (see fig. 22). The fact that the Fe/P ratios do not fall below these values suggests that the adsorption of phosphorus by ferric oxy-hydroxides is ultimately limited by the stoichiometry of tinticite and cacoxenite.

Thermodynamic calculations indicate that ferric oxy-hydroxides, which appear to be primarily responsible for phosphorus adsorption by bottom sediments, also control the precipitation of vivianite. When ferric oxy-hydroxides are present, they appear to adsorb

dissolved phosphate and form ferric phosphate phases to the exclusion of vivianite. The low concentrations of these compounds in the dredge spoil at site 5 appears to favor vivianite formation, however.

Figure 25 shows a plot of ferrous iron and phosphate activities in the pore waters of sediments at four sites in the study area, together with data from several other cores from the tidal river. The stability field boundaries for vivianite and caoxenite were calculated for a pH of 7.0 and for Eh values of −100 to +100 mV. The cacoxenite field boundaries were calculated from the formation reaction

$$[4Fe^{2+} + 3PO_4^{3-} + 15H_2O = Fe_4(PO_4)_3(OH)_3 \cdot 12H_2O + 3H^+ + 4e^-]$$

using the estimated free energies reported by Nriagu and Dell (1974). The field boundaries for tinticite are not included in figure 25 because of their close proximity to the cacoxenite boundaries. Since the vivianite reaction is Eh independent, only one field boundary is plotted for this mineral.

With the exception of two intervals from site 15, data points plot either within or close to the stability field for cacoxenite at sites 13, 14, and 15 and also at the other tidal river sites. For these cores, the plot indicates that the phosphate and iron activities are controlled by the precipitation of cacoxenite and/or tinticite. The data points from core 5A, however, fall well below the stability field for cacoxenite and much closer to the equilibrium activities for vivianite. The depletion of these sediments in ferric oxy-hydroxides, in combination with reducing conditions, favors the formation of vivianite over the formation of cacoxenite or tinticite.

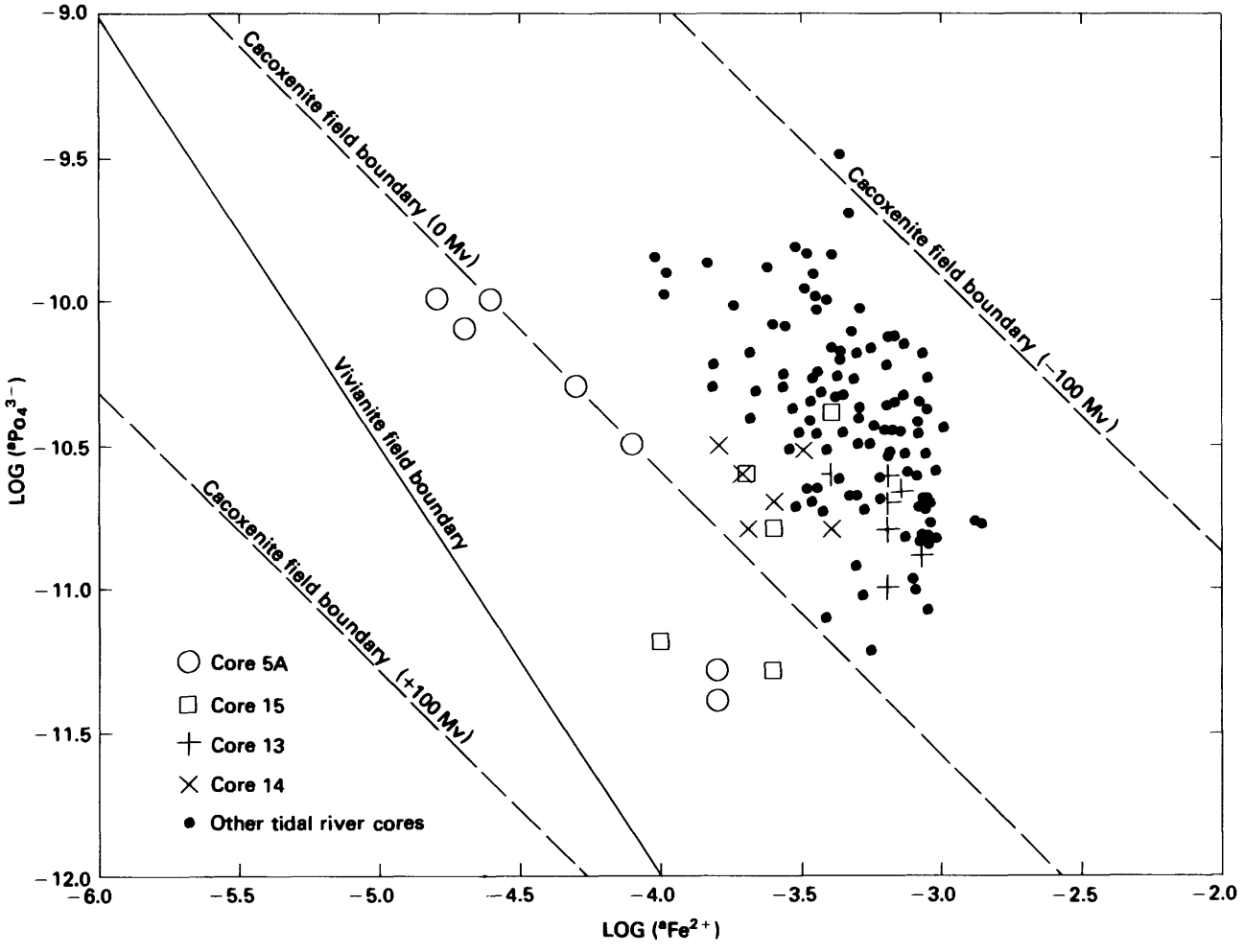

Figure 25. Activity diagram for Fe^{2+} and PO_4^{3} in sediment pore waters at stations 5, 13, 14, and 15 and other locations in the tidal Potomac (from Hearn and others, 1983).

Decay Constant of Dissolved Phosphorus in the Water Column

Even though the adsorption of dissolved phosphorus by suspended sediments probably involves more than one reaction, it can be approximated mathematically by describing the primary component reaction with a first-order or linear equation (Thomann, 1972), where the time rate of mass change is proportional to the mass itself times some linear rate coefficient.

In simple terms:

$$dc/dt = \pm Kc \,(K \geq 0) \qquad (1)$$

where c = solute concentration, t = time, and K = linear rate coefficient. The sign on K is positive when mass is gained and negative when mass is lost.

One way of obtaining the rate coefficient is through the solution to the idealized one-dimensional, steady-state transport equation (O'Conner, 1965):

$$C = \frac{M}{AU\sqrt{1+\alpha}} \exp \frac{Ux}{2E_x}(1 \pm \sqrt{1+\alpha}) \,, \qquad (2)$$

C = solute concentration,
x = distance in the seaward direction,
K = linear rate coefficient,
M = mass discharge rate at source,
U = advective velocity in the x direction,
E_x = cross-sectional area, and
$\alpha = \frac{4KE_x}{U^2}$

For tidal flow, a minus sign is used for $x > 0$ (seaward direction) and a plus sign is used for $x < 0$ (landward direction).

For the case of seaward transport, the expression within the brackets in equation 2 can be rewritten:

$$\frac{Ux}{2E_x}(1-\sqrt{1+\alpha}) = \frac{Ux\left(\frac{2K}{U^2}\right)}{2E_x\left(\frac{2K}{U^2}\right)}(1-\sqrt{1+\alpha}).$$

Multiplying both numerator and denominator by the quantity $\frac{2K}{U^2}$, we have

$$\frac{\frac{2Kx}{U}}{\alpha}(1-\sqrt{1+\alpha}) = \frac{-Kx}{U}\left[\frac{2}{\alpha}\left(\sqrt{1+\alpha}-1\right)\right].$$

In most cases the quantity α is negligibly small (Fischer, 1973).

Through a binomial expansion, the quantity $\left[\frac{2}{\gamma}\left(\sqrt{1+\gamma}-1\right)\right]$ approaches the value of 1. Therefore,

$$\frac{-Kx}{U}\left[\frac{2}{\alpha}\left(\sqrt{1+\alpha}-1\right)\right] = \frac{-Kx}{U} = -Kt = -K\bar{T},$$

where $\bar{T}$ = mean residence time as defined in appendix 1. For $\alpha \ll 1$, the expression $\frac{M}{AU\sqrt{1+\alpha}}$ is equivalent to the solute concentration C, leaving us with the final equation

$$C_t = C_0 e^{-Kt}, \qquad (3)$$

where C_0 = solute concentration at time = 0 and C_t = solute concentration at time = t.

Equation 3 must be corrected for the effects of dilution by incorporating a coefficient that is referenced to some conservative component in the effluent. Dissolved chloride serves this purpose well, since it behaves conservatively and its concentration in the effluent is greater than five times normal levels for the tidal river. The coefficient of dilution is calculated using the equation

$$\gamma = \frac{Cl_t - Cl_b}{Cl_0 - Cl_b} \qquad (4)$$

where γ = coefficient of dilution, Cl_t = the observed chloride concentration at the sample point, Cl_0 = the concentration of chloride in the effluent, and Cl_b = the background concentration of chloride in the river water.

Thus, undiluted effluent would yield a gamma value of 1.0, a 50/50 mixture of river water and effluent would have a gamma of 0.5, and river water containing no effluent would have a gamma of 0.0. Adding the dilution coefficient to equation 4, we have

$$C_t = C_0 \gamma e^{-Kt}. \qquad (5)$$

After substituting the terms P_0 (effluent dissolved phosphorus concentration) and P_t (dissolved phosphorus concentration at the sample point) for C_0 and C_t, and inserting a term, P_b, for the background concentration of dissolved phosphorus in the river, the equation becomes

$$P_t = [(P_0 - P_b)\,\gamma e^{-K\bar{T}}] + P_b. \qquad (6)$$

Rearranging and solving for K, the final form of the equation is

$$K_p = \frac{\ln\left[\frac{P_t - P_b}{(P_0 - P_b)\gamma}\right]}{\bar{T}} \qquad (7)$$

The linear decay constant K_p will reflect the cumulative effect of all processes that remove or add dissolved phosphorus to the water column. Biologic uptake, inorganic adsorption reactions with suspended and bottom sediments, and the precipitation of phosphate minerals are all capable of removing dissolved phosphorus under certain conditions. Unfortunately, for a single K_p value computed at a given location and time, it is not generally possible to resolve the relative importance of these processes. By computing K_p values at closely spaced intervals over a period of time, however, the nature of the components may be reflected in the variation of K_p with time.

Using the observed dissolved phosphorus and chloride values for each sample and for the effluent, and the mean residence time for the sampling station, K_p values were computed for 72 samples at stations B, C, D, and E. Data used in these computations are given in appendix 2. To simplify the calculations, average values for dissolved phosphorus and chloride in the effluent were used. The error introduced by this simplification was estimated using the observed variation of these parameters and should not exceed 0.2 units of K_p.

Values of K_p are consistently positive at all four stations, with the exception of a few samples collected at station E (fig. 26); this indicates that dissolved phosphorus was being removed from the water column in the embayment throughout the sampling period. Variations in K_p at each station exhibit a roughly diurnal periodicity; values show a rapid increase in phosphorus removal from noon to midnight, followed by a gradual dropoff in the removal rate from midnight to noon.

The most reasonable explanation of the periodicity shown by K_p values is the activity of photosynthetic organisms in the water column. This interpretation is supported

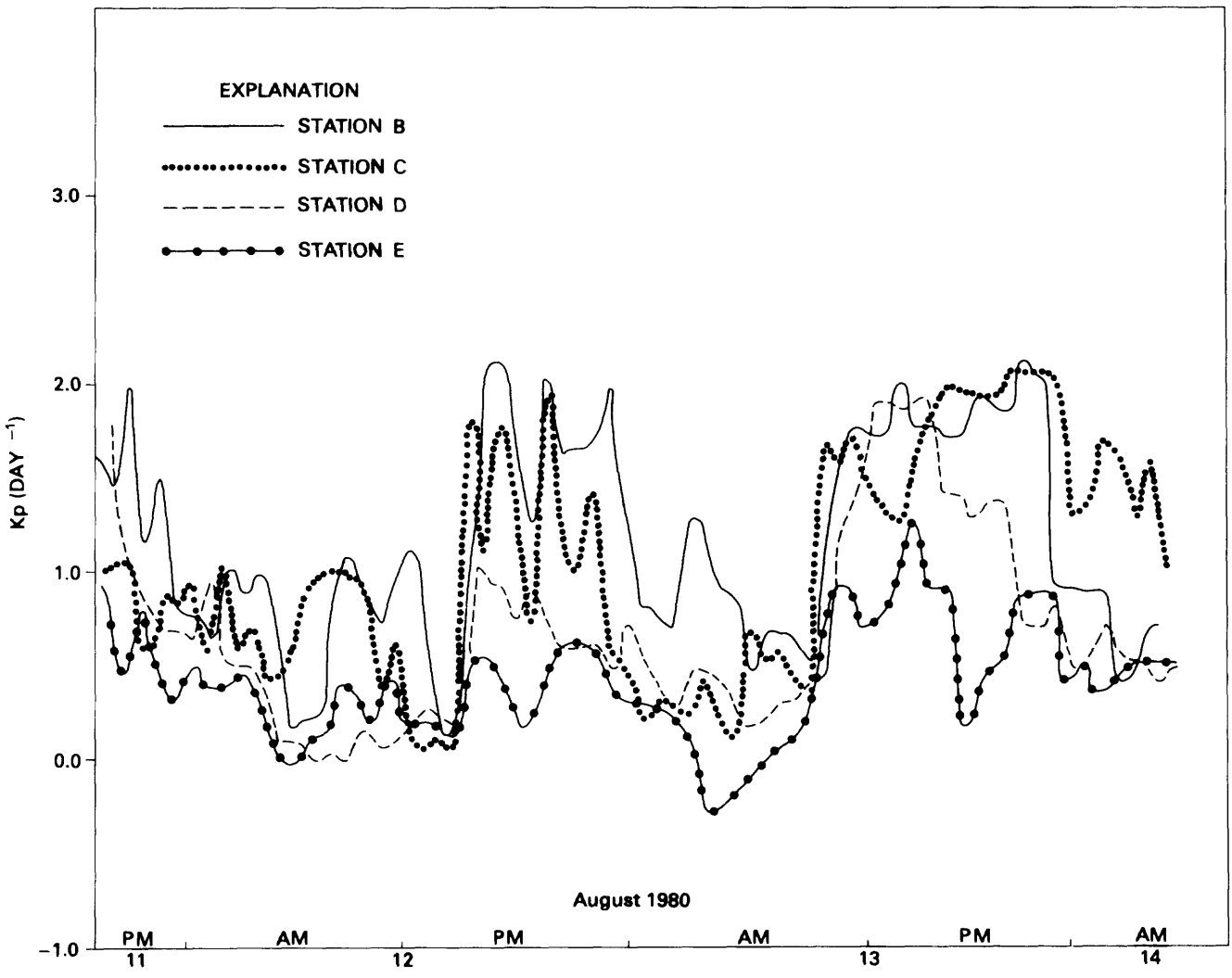

Figure 26. Time plot of the linear decay constant K_p for dissolved phosphorus at automatic-sampler stations B, C, D, and E during the period August 11-14, 1980.

by data collected 1 month earlier at a point approximately 15 miles downriver from the study area (Wayne Webb, unpub. data). Consistent and correlative diurnal variations in surface-water dissolved oxygen, pH, and temperature are clearly visible (fig. 27). The temperature record reflects the thermal effects of changes in light intensity. Variations in light intensity are in turn responsible for the metabolic production of oxygen by photosynthetic organisms, which causes the observed oxygen excursions. The regular 24-hour periodicity of these data agree well with the period observed for the decay constant, K_p. The correlation of pH maxima with temperature and oxygen highs is consistent with the increased consumption of CO_2 by phytoplankton. This phenomenon may have a significant influence on the availability of dissolved phosphorus. The adsorption capacity of the oxides and hydroxides of iron and aluminum, as well as most of the clay minerals, are known to decrease with increasing pH. The substantial increases in pH (as much as 1 unit) associated with algal activity could conceivably cause the desorption of phosphorus from suspended sediments, thereby increasing the availability of this nutrient. Although it is not possible to verify this desorption or to determine its magnitude without further experimentation, it is plausible that such a mechanism plays an important role in the metabolic utilization of adsorbed phosphorus.

As was noted above, the values of K_p reflect both cyclic removal of dissolved phosphorus by phytoplankton and noncyclic removal by inorganic adsorption. Average values of K_p for stations B, C, D, and E were computed by summing individual values over a 48-hour period and dividing by the number of measurements. The average values of K_p for stations B, C, D, and E were 1.22, 1.06, 0.70, and 0.40 per day, respectively (fig. 28). The data from station E probably reflect the mixing of embayment water with effluent-free water that traveled down the main channel. For this reason, the best estimate of the average K_p for the entire embayment probably lies somewhere between the values obtained for stations D and E. The progressive increase of K_p with increasing distance from the outfall suggests that the removal rate is affected by the concentration of dissolved phosphorus. This is consistent with observations of concentration dependence in studies of both inorganic (Krom and Berner, 1980; Lake and MacIntyre, 1977) and organic uptake of dissolved phosphorus (Vollenweider, 1968; Young and King, 1980).

Total Mass of Effluent-Derived Phosphorus in Embayment Sediments

Sediments in the embayment have been shown to be enriched in total phosphorus to a depth of 10–20 cm. Concentrations of total phosphorus in sediments below this depth are substantially lower and show only minor variation. Profiles of dissolved phosphorus in sediment pore

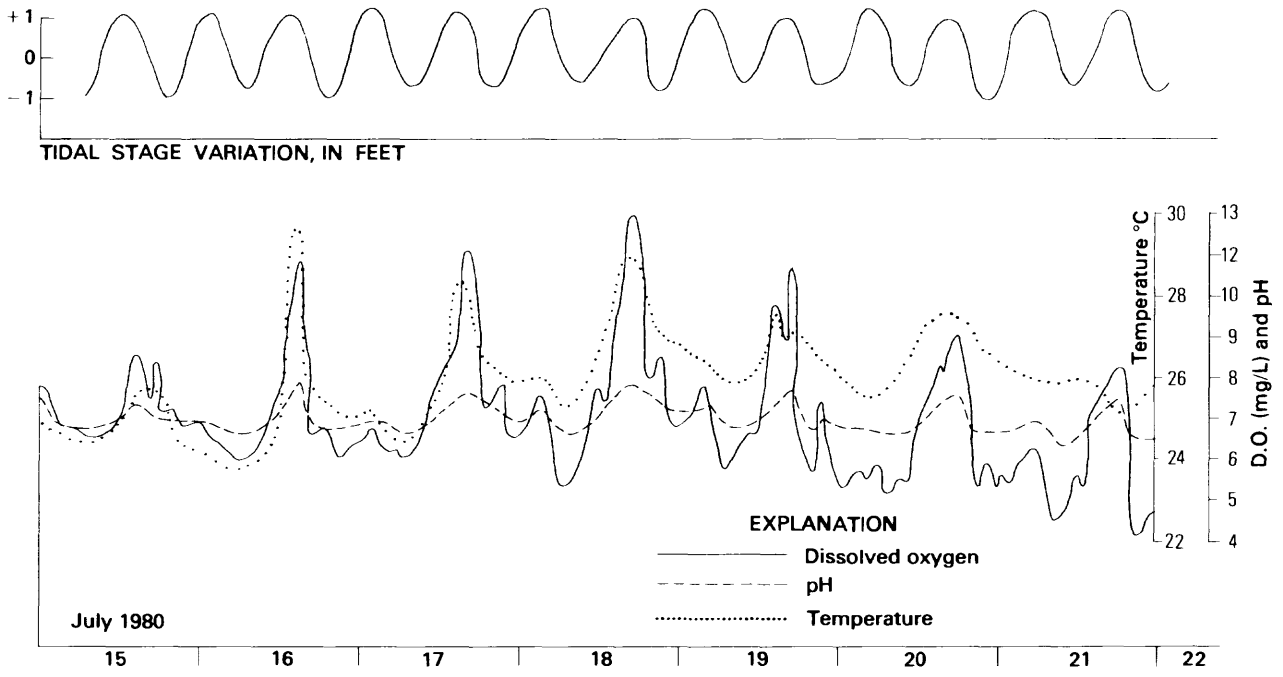

Figure 27. Time plots of surface-water dissolved oxygen, pH, and temperature in the Potomac River near Indian Head, Md., for the period July 15–21, 1980 (reproduced from unpublished data of Wayne Webb, USGS).

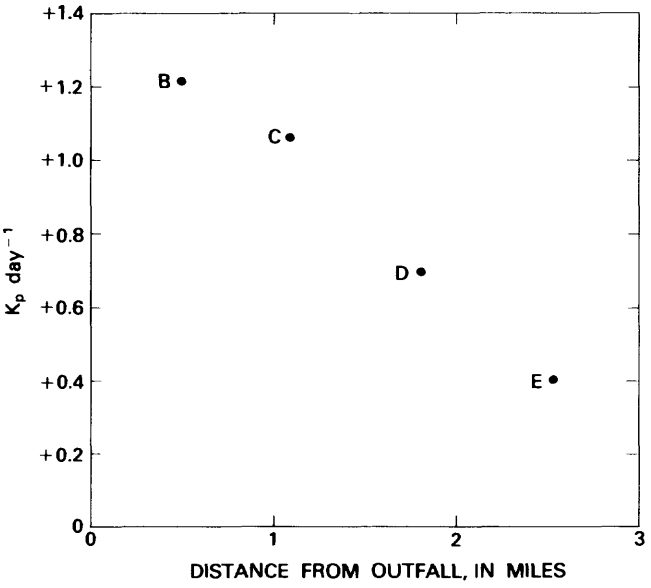

Figure 28. Plot of 48-hour averaged K_p values for stations B, C, D, and E versus distance from the outfall.

waters do not indicate significant mobilization and upward diffusion of phosphorus; it appears, rather, that the high concentrations of total phosphorus in surface sediments are due primarily to the deposition of suspended sediments enriched in phosphorus from contact with effluent. If this hypothesis is valid, the mass of effluent-derived phosphorus that has been retained in the embayment can be estimated through a few simple calculations. A background level of total phosphorus was estimated for each core from the average concentration of intervals below 20 cm depth. This value was subtracted from the phosphorus-enriched intervals above 20 cm in depth. The net concentrations were integrated vertically in each core to yield an average figure for the weight percent phosphorus attributable to an effluent source. The total mass of effluent-derived phosphorus was estimated by dividing the embayment into six subareas, extrapolating the concentration and porosity values for each core, and then summing.

The total mass of effluent-derived phosphorus obtained from the above computations is 2.4×10^5 kg. Treatment plant records indicate that approximately 1.8×10^6 kg of phosphorus was discharged from the time the current outfall was installed in 1977 until the collection of the cores in 1980. The estimated mass of effluent-derived phosphorus within the embayment represents approximately 13 percent of this value.

Measurements of phosphate sedimentation and benthic flux elsewhere in the tidal Potomac River suggest that most of the phosphorus input to bottom sediments in the embayment is retained there. Callender (1982) reported that only 10 to 20 percent of the phosphorus sedimented in the tidal river was released back into the water column.

SUMMARY AND CONCLUSIONS

The mobility of phosphorus discharged into the Potomac River from the Blue Plains wastewater treatment plant has been shown to be influenced by both the hydrodynamics and the geochemistry of the tidal-river environment. The most important control on phosphorus transport is a bathymetric feature. The removal of substantial quantities of sand and gravel from the eastern shore of the river in the early 1900's, followed by the dumping of dredge spoil in a midriver shoal area, created a restricted embayment which is protected from discharge variations in the main channel and is flushed largely by tidal action. This embayment serves as an effective sediment trap, especially during periods of high flow, when large quantities of suspended sediment from the main channel are transported into it by flood tides.

The site at the head of the embayment, chosen for the installation of a new outfall in 1977, has caused the flow of effluent to be effectively restricted to the embayment until it joins the main channel 4 km below the outfall. Measurements of mean residence time indicate that a period of approximately 2½ days is required for effluent to travel from the outfall to the embayment mouth. This configuration has facilitated the accumulation of substantial quantities of phosphorus adsorbed from solution by sediments within the embayment area. Approximately 13 percent of the phosphorus discharged by the treatment plant from September 1977 to August 1980 is estimated to have been retained in the embayment sediments.

The adsorption of phosphorus from solution is accomplished primarily through the action of suspended sediments, and to a lesser degree by bottom sediments. Measurements of a linear decay constant reflect a diurnal cycling of phosphorus within the water column by phytoplankton, which correlates with diurnal variations in dissolved oxygen, pH, and temperature observed elsewhere in the tidal river. This cyclic uptake and release is superimposed on a relatively constant level of removal, which is attributed to inorganic adsorption mechanisms.

The amorphous oxy-hydroxides of iron, the ferrous phosphate mineral vivianite, and, to a lesser extent, amorphous aluminum are the primary inorganic phosphate-containing phases in the sediments within the study area. This conclusion is supported by data from pore-water analyses, thermodynamic calculations, ammonium-oxalate extractions, and measurements of phosphate-adsorption capacity. Oxalate-extractable iron is present in sufficient quantities to coordinate all of the phosphorus present in bottom sediments. Levels of extractable aluminum are lower than levels of extractable iron by a factor of six or more. The role of clay minerals in the adsorption process appears to be minor; they serve primarily as a substrate for the accumulation of oxy-hydroxide phases. Low levels of ferric oxy-hydroxides and more reducing conditions in the coarse

dredge-spoil sediments of the upper portion of the embayment have apparently caused the precipitation of vivianite.

The enrichment of sediments close to the outfall in amorphous iron and aluminum indicates that particulate iron and aluminum have been discharged with the effluent. These compounds are apparently the residual of ferric chloride, ferrous sulfate, and aluminum sulfate used in the phosphorus-removal process. Although the use of aluminum has been minimal, more than 5×10^6 kg of iron are estimated to have been discharged through the outfall since its installation in 1977.

The level of phosphorus saturation, indicated by the ratio of oxalate-extractable iron to extractable phosphorus, decreases rapidly with distance from the outfall; sediments in the lower portions of the embayment are close to values typical for tidal-river sediments several miles downriver. Thermodynamic calculations and extractable Fe/P ratios of phosphorus-saturated sediments indicate that adsorption is ultimately limited by the stoichiometry of ferric phosphate minerals. These phases are the stable end products of phosphating ferric oxy-hydroxides.

REFERENCES CITED

Barth, T. F. W., 1937, Crystallographic studies in the vivianite group: Am. Mineralogist, v. 22, p. 325–341.

Bergman, J. G., and Savik, J., 1957, Anal. Chemistry, v. 29, p. 241.

Black, C. A., 1968, Soil-plant relationships: New York, John Wiley.

Callender, E., 1982, Benthic phosphorus regeneration in the Potomac River estuary: Hydrobiologia, v. 92, p. 431–446.

Carroll, D., 1958, Role of clay minerals in the transportation of iron: Geochim. et Cosmochim. Acta, v. 14, p. 1–27.

———1970, Clay minerals: A guide to their X-ray identification: Geological Society of America Special Paper 126, 80 p.

Dana, E. S., 1950, A textbook of mineralogy (4th ed.): New York, John Wiley, 851 p.

District of Columbia, Department of Environmental Services, 1974, Wastewater Treatment Plant of the District of Columbia, Government of the District of Columbia Department of Environmental Services, Brochure ES–6.

Edzwald, J. D., Toensing, D. C., and Leung, M. C.-Y., 1976, Phosphate adsorption reactions with clay minerals: Environmental Sci. and Technology, v. 10, p. 485–490.

Einsele, W., 1938, Uber chemische und kolloid-chemische Vorgange in Eisenphosphat-systemen unter limnochemischen und limnogeologischen Geseichtspunken: Arch. Hydrobiol. 33, p. 361–387.

Fischer, H. B., 1973, Longitudinal dispersion and turbulent mixing in open-channel flow, *in* Van Dyke, M., Vincenti, W. G., and Wehausen, J. V., eds., Annual review of fluid mechanics, v. 5: Palo Alto, Calif., Annual Reviews Inc., 443 p.

Garrels, R. M., and Christ, C. L., 1965, Solutions, minerals, and equilibria: San Francisco, Freeman, Cooper and Company, 450 p.

Hearn, P. P., Parkhurst, D. L., and Callender, E., 1983, Authigenic vivianite in Potomac River sediments: Control by ferric-oxyhydroxides: Jour. Sed. Petrology, v. 53, no. 1, p. 165–177.

Hemwall, J. B., 1957a, The fixation of phosphorus by soils: Adv. Agron., v. 9, p. 95–112.

———1957b, The role of soil clay minerals in phosphorus fixation: Jour. Soil Sci., v. 83, p. 101–108.

Hingston, F. J., Posner, A. M., and Quirk, J. P., 1974, Anion adsorption by goethite and gibbsite. 2. Desorption of anions from hydrous oxide surfaces: Jour. Soil Sci., v. 25, p. 16–26.

Hubbard, E. F., and Stamper, W. G., 1972, Movement and dispersion of soluble pollutants in the Northeast Cape Fear Estuary, North Carolina: U.S. Geol. Survey Water-Supply Paper 1873-E, 31 p.

James, H. L., 1966, Chemistry of the iron-rich sedimentary rocks, ch. W *in* Fleischer, M., ed., Data of geochemistry (6th ed.): U.S. Geol. Survey Prof. Paper 440-W, 61 p.

Jenne, E. A., 1977, Trace element sorption by sediments and soil—Sites and processes: *in* Chappel, W., and Petersen, K., eds., v. 2., Symposium on molybdenum in the environment: New York, M. Dekker, Inc.

Jennings, D. S., 1919, The effect of certain colloidal substances on the growth of wheat seedlings: Jour. Soil Sci., v. 7, p. 201–215.

Jitts, H. R., 1959, The adsorption of phosphate by estuarine bottom sediments: Aust. Jour. Marine Freshwater Research, v. 10, p. 7–21.

Khalid, R. A., Patrick, W. H., and Delaune, R. D., 1977, Phosphorus sorption characteristics of flooded soils: Jour. Soil Sci., v. 41, p. 305–310.

Kilpatrick, F. A., 1972, Automatic sampler for dye tracer studies: Water Resources Research, v. 8, no. 3, p. 737–745.

Krom, M. D., and Berner, R. A., 1980, Adsorption of phosphate in anoxic marine sediments: Limnol. Oceanogr., v. 25, no. 5, p. 797–806.

Lake, C. A., and MacIntyre, W. G., 1977, Phosphate and tripolyphosphate adsorption by clay minerals and estuarine sediments: Virginia Water Resources Research Center Bulletin 109 (Virginia Polytechnic Institute and State University, Blacksburg).

Larsen, S., 1967, Soil phosphorus: Adv. Agron., v. 19, p. 131–210.

Laverty, J. C., and Mclean, E. O., 1961, Jour. Soil Sci., v. 91, p. 166–171.

Li, W. C., Armstrong, D. E., Williams, J. D., Harris, R. F., and Syers, J. K., 1972, Rate and extent of inorganic phosphate exchange in lake sediments. Soil Sci. Soc. Am. Proc. 36: p. 279–285.

McCallister, D. L., and Logan, T. J., 1978, Phosphate adsorption-desorption characteristics of soils and bottom sediments in the Maumee River Basin of Ohio: Jour. Environmental Quality, v. 7, no. 1, p. 87–92.

Mortimer, C. H., 1941, The exchange of dissolved substances between mud and water in lakes: Jour. Ecology, v. 29, p. 280–329.

Muljadi, D., Posner, A. M., and Quirk, J. P., 1966, The mechanism of phosphate adsorption by kaolinite, gibbsite, and pseudoboehmite. 1. The isotherms and the effect of pH on adsorption: Jour. Soil Sci., v. 17, p. 212–229.

Murphy, J., and Riley, J. P., 1962, A modified single solution method for the determination of phosphate in natural waters: Anal. Chim. Acta., v. 27, p. 31–36.

Nriagu, J. O., and Dell, C. I., 1974, Diagenetic formation of iron phosphates in recent lake sediments: Am. Mineralogist, v. 59, p. 934–946.

O'Conner, D. J., 1965, Estuarine distribution of nonconservative substances: Jour. Sanit. Eng. Div. Proc. ASCE91(SA1): p. 23–42.

Parfitt, R. L., 1977, Phosphate adsorption on an oxisol: Jour. Soil Sci., v. 41, p. 1046–1067.

Parfitt, R. L., Atkinson, R. J., and Smart, R. St. C., 1975, The mechanism of phosphate fixation by iron oxides: Jour. Soil Sci., v. 39, 837–841.

Pierce, J. W., 1974, Suspended and bottom sediments of the Rhode River, *in* Chesapeake Research Consortium Annual Technical Report to NSF/RANN, grant G138973.

Piercey, E. J., 1981, Phosphate sorption on clay-rich channel sediments of the tidal Potomac River and estuary: Abstracts to the sixth biennial conference of the Estuarine Research Federation, *in* Estuaries, v. 4, no. 3, p. 251.

Pomeroy, L. R., Smith, E. E., and Grant, C. M., 1965, The exchange of phosphate between estuarine water and sediments: Limnol. Oceanogr. 24: p. 356–364.

Reeburgh, W. S., 1967, An improved interstitial water sampler: Limnol. and Oceanogr., v. 12, p. 163–165.

Rose, H. J., Adler, I., and Flanagan, F. J., 1962, Use of La_2O_3 as a heavy absorber in the X-ray fluorescence analysis of silicate rocks: U.S. Geol. Survey Prof. Paper 450–B, p. 80–82.

Ryden, J. C., McLaughlin, J. R., and Syers, J. K., 1977, Mechanisms of phosphate sorption by soils and hydrous ferric oxide gel: Jour. Soil Sci., v. 28, p. 72–92.

Saunders, W. M. H., 1964, Phosphate retention by New Zealand soils and its relationship to free sesquioxides, organic matter, and other soil properties: New Zealand Jour. of Agricultural Research, v. 8; p. 30–57.

Schwertmann, U., 1964, Differentiation of the iron oxides of the soil by extraction with ammonium-oxalate solution: Z. PflErnahr. Dung., v. 105, p. 194–202 [translated by Liska Snyder, 1967].

Schwinn, D. E., and Tozer, G. K., 1974, Largest advanced wastewater treatment plant in the U.S., and in the world: Env. Sci. and Technology, v. 8, p. 892–897.

Skougstad, M. W., Fishman, M. J., Friedman, L. C., Erdman, D. E., and Duncan, S. S., eds., 1979, Methods for determination of inorganic substances in water and fluvial sediments: Techniques of Water Resource Investigations for the U.S. Geol. Survey, Bk. 5, Chap. A1.

Smart, P. L., and Laidlaw, I. M. S., 1977, An evaluation of some fluorescent dyes for water tracing: Water Resources Research, v. 13, no. 1, p. 15–33.

Thomann, R. V., 1972, Systems analysis and water quality management: New York, Environmental Research and Applications, Inc., 286 p.

Veith, J. A., and Sposito, G., 1977, Reactions of aluminosilicates, aluminum hydrous oxides, and aluminum oxide with o-phosphate: The formation of X-ray amorphous analogs of variscite and montebrasite: Jour. Soil Sci., v. 41, p. 870–876.

Volk, V. V., and Mclean, E. O., 1963, Jour. Soil Sci., v. 27, p. 53–58.

Vollenweider, R. A., 1968, Scientific fundamentals of the eutrophication of lakes and flowing waters, with particular reference to nitrogen and phosphorus as factors in eutrophication: Organisation for Economic Co-operation and Development, DAS CSI 68, v. 27.

Way, J. T., 1850, On the power of soils to absorb manure: Jour. of the Royal Agricultural Society, v. 11, p. 313–379.

Williams, J. D. H., Syers, J. K., Shukla, S. S., and Harris, R. F., 1971, Levels of inorganic and total phosphorus in lake sediments as related to other sediment parameters: Environmental Sci. and Technology, v. 5, p. 1113–1120.

Young, T. C., and King, D. L., 1980, Interacting limits to algal growth: Light, phosphorus, and carbon dioxide availability: Water Research, v. 14, p. 409–412.

Yotsukura, N., 1968, Discussion of "Longitudinal mixing in natural streams," by E. L. Thackston and P. A. Krenkel: Jour. of the Sanitary Engineering Division, ASCE, v. 94, p. 568–571.

Yotsukura, N., and Kilpatrick, F. A., 1973, Tracer simulation of soluble waste concentration: American Society of Civil Engineers, Jour. of Environmental Engineering Division, v. 99, no. EE4, p. 499–516.

APPENDIX 1: DETERMINATION OF MEAN RESIDENCE TIME BY THE METHOD OF LINEAR SUPERPOSITION

The principle of linear superposition has been most commonly used to determine the long-term equilibrium concentration of a solute discharged into a body of water by "superposing" the data from a short-term dye injection (Hubbard and Stamper, 1972; Yotsukura, 1968). The technique is also amenable to the determination of mean residence time, however, and it is this application that is described here.

The method is best explained by using a hypothetical example. Suppose a quantity of dye tracer is injected into an effluent stream just before it enters some body of water with a tidal flow regime. The dye is injected at a constant rate beginning at low slack tide, continuing through the next low tide, and ending at the second low slack tide. This time period P would be 1 tidal day and would equal twice the tidal period of the system. At some point downstream from the outfall, dye concentrations are monitored constantly in order to yield a time-response curve. This response curve should consist of several peaks and valleys, with the distance between successive peaks being equal to $P/2$ (figure 29a). The midpoint of the injection period is labeled T_0, and the time after which no dye is detected at the sample point is labeled T_{max}, T_{max} being equivalent to the flushing time. If all the dye passes the sample point within one tidal day, 1 to 3 peaks will appear on the response curve. More commonly, however, it will take much longer than P hours for the dye to pass the sampling point. In this case there will be several peaks, which increase in magnitude until the center of the dye cloud passes the sample point and then decrease until the entire cloud has passed the point.

The response to an injection period much longer than P hours can be visualized as a string of simultaneous $1P$ injections. For example, if the injection period were increased to $7P$ hours, the dye concentration (S) one would expect to observe at the sample point at the end of the injection at time T_s could be represented as the summation of the individual concentrations (S_i's) resulting from a series of seven single discharges each P hours long (figure 29b). There should be no dye present at the sample point from the first three periods of the discharge interval, because the time difference between T_s and these periods is greater than the flushing time, T_{max}. All of the dye from these periods will have already passed the sample point. Some dye from each of the fourth through seventh periods should still be present, however. The quantity of dye at the sample point from each period can be determined by measuring the time difference between the center of the given period and T_s (lower part of figure 29b) and then reading the concentration from the single period response curve at that time difference from T_0 (upper part of figure 29b). Thus, the amount of dye at the sample point that was released during period T_4 would equal the quantity S_4. If one repeats this procedure for all the periods, the total concentration at the sample point will be represented by the summation

$$S = \sum_{i=4}^{7} S_i. \tag{1}$$

Since the dye concentration at the sample point at time T_s is the sum of all the component S_i's, each of which has a residence time T_i, the mean residence time for the total concentration S is an average that can be computed from the equation

$$\overline{T} = \frac{\sum_{i=4}^{7} S_i T_i}{\sum_{i=4}^{7} S_i}. \tag{2}$$

The general form of this equation would be

$$\overline{T} = \frac{\sum_{i=-\infty}^{\infty} S_i T_i}{\sum_{i=-\infty}^{\infty} S_i}. \tag{3}$$

Using equation 3, mean residence time can be computed from the response curves of dye concentration by reading the dye concentration (S_i) every P hours from time T_0 until no more dye is detectable (S_i=0).

It can be seen from this example that the dye concentration at the sample point at each time T_i can vary, depending on the phase relation of T_i to the tidal stage within the period P. The maximum concentrations will be obtained by shifting the initial T_s by some fraction of P so that the T_i's correspond to the peak concentrations of the response curve.

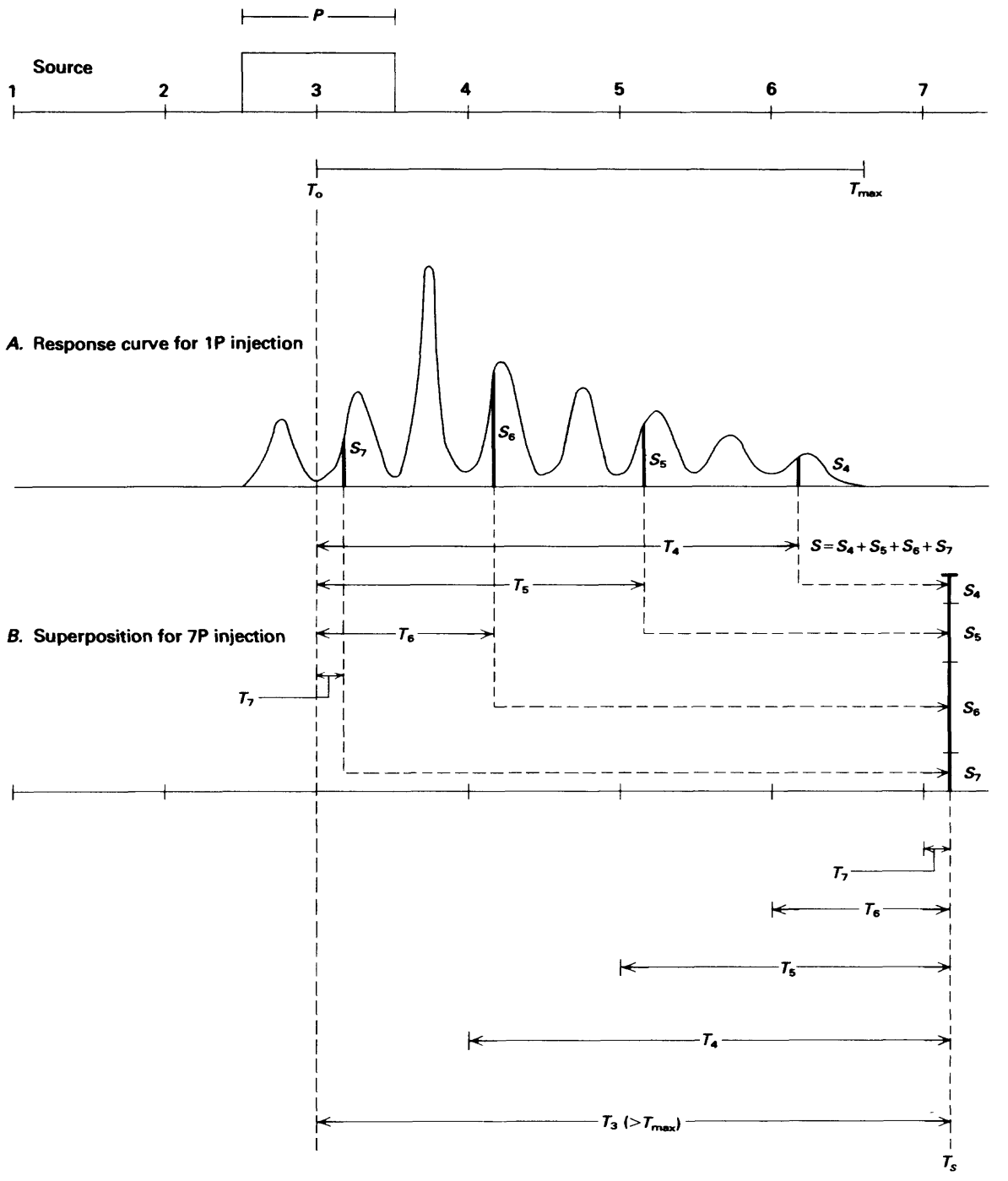

Figure 29. Hypothetical response curve from a 1 tidal-day dye injection illustrating the calculation of mean residence time by the method of linear superposition. See text for explanation of symbols.

APPENDIX 2: AUTOMATIC SAMPLER DATA

Sample No.	Time	Dye (ppb)	Dissolved PO_4 (ppb)	Chloride (ppm)
Sampler A				
	8/11/80			
A1-2	0012	0.1	---	---
4	0154	0.1	---	---
6	0336	0.2	---	---
8	0512	0.1	---	---
10	0654	0.1	---	---
12	0836	0.1	---	---
13	0924	0.1	---	---
14	1018	0.2	---	---
15	1106	0.5	---	---
16	1200	5.5	---	---
17	1248	1.7	---	---
18	1336	1.5	---	---
22	1700	2.2	---	---
A2-1	1836	4.0	31	24.8
2	1924	3.4	26	22.3
3	2012	2.7	10	21.1
4	2106	3.5	16	22.3
5	2154	3.7	41	20.7
6	2248	4.1	52	20.3
7	2336	9.2	98	24.8
	8/12/80			
8	0024	8.8	124	24.4
9	0118	10.4	140	24.4
10	0206	9.7	140	26.1
11	0300	10.2	170	25.7
12	0348	10.9	160	25.3
13	0436	9.0	108	26.6
14	0530	8.7	72	25.7
15	0618	5.2	41	24.0
16	0712	5.7	62	23.2
17	0800	6.6	72	21.9
18	0848	6.6	72	28.4
19	0942	1.5	88	21.1
20	1030	1.0	88	19.2
21	1124	0.5	88	18.4
22	1212	2.0	108	19.2
23	1300	2.2	134	22.7
24	1354	2.6	160	25.3
A3-1	1500	2.0	18	22.7
2	1548	2.4	7	23.6
3	1642	3.0	7	21.9
4	1730	3.0	5	21.1
5	1818	2.6	---	---
6	1912	2.6	7	23.6
7	2000	2.4	7	24.8
8	2054	2.5	7	22.3
9	2142	2.4	7	23.2
10	2230	1.6	13	20.3
11	2324	1.3	50	21.9
	8/13/80			
12	0012	1.3	97	21.9
13	0106	1.2	112	23.6
14	0154	1.1	165	26.1
15	0242	1.1	149	24.8
16	0336	1.0	202	26.6
17	0424	1.0	202	28.8
18	0518	1.0	260	29.8
19	0606	1.5	131	23.6
20	0672	1.4	65	23.6
21	0748	1.2	97	26.1
22	0848	1.1	202	27.5
23	0924	1.1	112	20.0
24	1018	---	---	---

Note: Entire A4 sequence of samples was lost because of failure of sampler gear drive.

	8/14/80			
A5-1	0900	0.4	---	---
3	1254	0.4	---	---
5	1700	0.3	---	---
7	2054	0.4	---	---
	8/15/80			
9	0100	0.3	---	---
11	0354	0.3	---	---
13	0800	0.3	---	---
15	1154	0.3	---	---
17	1600	0.2	---	---
19	1954	0.3	---	---
21	2400	0.3	---	---
	8/16/80			
23	0354	0.2	---	---
Sampler B				
	8/11/80			
B1-2	0012	0.1	---	---
4	0148	0.1	---	---
6	0336	0.1	---	---
8	0515	0.2	---	---
10	0700	0.1	---	---
12	0842	0.2	---	---
14	1024	0.2	---	---
16	1206	0.1	---	---
17	1300	0.8	---	---
18	1348	1.9	---	---
19	1442	2.4	---	---
21	1624	1.6	---	---
22	1712	0.5	---	---
23	1806	0.2	---	---
B2-1	1842	0.3	16	19.9
2	1930	0.2	21	19.9
3	2024	0.3	10	20.4
4	2112	0.4	31	19.6
5	2206	4.4	26	23.2

Sample No.	Time	Dye (ppb)	Dissolved PO_4 (ppb)	Chloride (ppm)
Sampler B—Continued				
6	2254	8.7	78	25.4
7	2348	6.4	62	24.1
	8/12/80			
8	0036	8.0	114	24.7
9	0130	5.1	52	24.1
10	0218	7.4	108	25.1
11	0312	7.8	93	24.7
12	0400	7.8	134	24.7
13	0454	6.9	124	24.7
14	0542	2.8	67	22.9
15	0636	3.9	52	22.5
16	0724	1.5	41	20.4
17	0818	1.6	41	20.2
18	0906	0.8	47	20.4
19	1000	8.7	150	25.4
20	1048	4.1	83	21.6
21	1142	1.0	123	18.7
22	1230	3.4	179	21.3
23	1324	3.2	187	22.9
24	1412	3.2	211	23.8
B3-1	1506	3.2	18	24.1
2	1600	2.4	49	23.5
3	1648	2.2	13	19.9
4	1742	1.3	23	20.4
5	1830	2.0	65	20.7
6	1924	2.8	13	23.8
7	2012	2.5	28	22.2
8	2106	2.5	28	21.6
9	2154	2.4	44	22.9
10	2248	1.5	91	24.7
11	2336	1.5	102	23.5
	8/13/80			
12	0030	1.3	107	22.5
13	0118	1.3	154	22.2
14	0212	1.2	154	24.1
15	0300	1.4	139	22.9
16	0354	1.4	165	23.8
17	0442	1.8	118	23.2
18	0536	1.7	160	23.8
19	0624	1.2	149	20.2
20	0718	1.3	81	22.9
21	0806	1.4	91	21.9
23	0948	1.3	86	21.9
24	1042	1.2	107	20.4
B4-1	1118	1.1	18	21.9
2	1212	1.2	24	22.2
3	1300	1.2	24	22.5
4	1354	1.0	29	24.4
5	1442	1.1	40	23.8
6	1536	1.0	40	24.4
7	1624	1.0	24	24.4
8	1718	1.1	18	24.1
9	1806	1.1	13	23.2
10	1900	1.2	13	22.9
11	1948	1.2	13	21.9
12	2042	1.5	13	21.9
13	2130	1.3	13	20.7
14	2224	1.3	8	19.9
15	2312	1.2	13	24.1
	8/14/80			
16	0006	1.0	71	26.4
17	0054	1.0	71	25.4
18	0148	1.0	66	23.8
19	0236	1.0	66	24.1
20	0330	0.8	145	26.0
21	0418	0.9	150	27.3
22	0512	1.5	103	26.7
23	0600	1.2	13	23.8
24	0654	1.1	40	23.5
B5-1	0854	0.4	---	---
2	1100	0.4	---	---
3	1254	0.4	---	---
4	1500	0.4	---	---
5	1654	0.4	---	---
6	1900	0.4	---	---
7	2054	0.4	---	---
8	2300	0.4	---	---
	8/15/80			
9	0054	0.3	---	---
10	0300	0.3	---	---
11	0454	0.3	---	---
12	0700	0.4	---	---
13	0854	0.3	---	---
14	1100	0.3	---	---
15	1254	0.3	---	---
16	1500	0.3	---	---
18	1900	0.3	---	---
19	2054	0.3	---	---
20	2300	0.3	---	---
	8/16/80			
21	0054	0.3	---	---
22	0300	0.2	---	---
23	0454	0.2	---	---
24	0700	0.2	---	---
Sampler C				
	8/11/80			
C1-2	0013	0.3	---	---
4	0154	0.4	---	---
6	0336	0.2	---	---
8	0518	0.2	---	---
10	0700	0.3	---	---
12	0842	0.4	---	---
13	0936	0.4	---	---
14	1024	0.0	---	---
15	1118	0.5	---	---
16	1206	0.4	---	---
17	1254	0.6	---	---
19	1436	0.3	---	---
20	1618	0.1	---	---

Sample No.	Time	Dye (ppb)	Dissolved PO_4 (ppb)	Chloride (ppm)
	Sampler C — Continued			
21	1712	0.3	—	—
22	1800	0.1	—	—
C2-1	1854	0.3	35	22.9
2	1942	0.2	43	24.9
3	2036	0.2	83	23.9
4	2124	0.3	83	23.5
5	2218	0.2	51	23.2
6	2306	0.3	59	23.2
7	2400	2.5	75	25.9
	8/12/80			
8	0048	4.3	99	27.3
9	0142	1.6	51	26.2
10	0230	2.8	59	25.5
11	0324	3.0	51	25.9
12	0412	4.9	75	25.5
13	0506	2.0	171	23.2
14	0554	3.0	147	22.6
15	0648	0.9	131	22.2
16	0736	1.0	43	22.5
17	0824	1.1	35	22.5
18	0918	1.0	51	22.5
19	1006	1.2	67	22.9
20	1100	1.1	35	22.9
21	1148	2.3	35	23.5
22	1242	4.7	99	24.2
23	1330	3.2	171	22.5
24	1424	3.5	131	23.9
C3-1	1524	3.0	13	23.5
2	1612	2.8	7	23.2
3	1706	2.5	7	23.9
4	1754	2.7	13	23.5
5	1848	2.7	28	22.9
6	1936	0.8	7	20.6
7	2030	0.7	13	21.6
8	2118	1.8	13	22.2
9	2212	2.0	13	22.9
10	2300	1.4	7	21.3
11	2354	1.6	23	21.6
	8/13/80			
12	0042	2.4	65	24.9
13	0136	1.9	65	24.9
14	0224	1.8	76	24.2
15	0318	1.7	28	24.5
16	0406	1.7	44	22.5
17	0454	1.9	55	23.5
18	0548	1.7	97	22.9
19	0636	1.3	60	21.3
20	0730	1.8	65	21.9
21	0818	1.3	65	21.3
22	0912	1.3	81	21.6
23	1000	1.4	60	21.9
24	1054	1.4	18	24.2
C4-1	1136	1.4	18	24.2
2	1230	1.4	13	24.5
3	1318	1.3	13	24.2
4	1412	1.5	13	23.5
5	1500	1.3	8	23.5
6	1554	1.2	13	24.5
7	1642	1.2	13	24.5
8	1736	1.2	13	23.5
9	1824	1.2	13	22.9
10	1918	1.3	8	21.3
11	2006	1.4	8	21.6
12	2100	1.4	8	24.9
13	2148	1.3	8	24.9
14	2242	1.3	8	24.2
15	2330	1.2	8	24.5
	8/14/80			
16	0024	1.3	8	23.5
17	0112	1.2	24	22.5
18	0200	1.1	24	23.5
19	0254	1.2	13	22.9
20	0342	1.2	13	22.9
21	0436	1.1	24	21.9
22	0524	1.1	13	21.3
23	0618	1.0	29	21.6
24	0706	1.1	8	21.9
C5-1	0900	0.5	—	—
2	1054	0.5	—	—
3	1300	0.5	—	—
4	1454	0.5	—	—
5	1700	0.4	—	—
6	1854	0.4	—	—
7	2100	0.4	—	—
8	2254	0.4	—	—
	8/15/80			
9	0100	0.5	—	—
10	0254	0.4	—	—
11	0500	0.4	—	—
12	0654	0.4	—	—
13	0900	0.4	—	—
14	1054	0.4	—	—
15	1300	0.3	—	—
16	1454	0.3	—	—
17	1700	0.3	—	—
18	1854	0.3	—	—
19	2100	0.2	—	—
20	2254	0.2	—	—
	8/16/80			
21	0100	0.2	—	—
22	0254	0.2	—	—
23	0500	0.2	—	—
24	0654	0.2	—	—
	Sampler D			
	8/11/80			
D1-2	0018	0.1	—	—
4	0206	0.2	—	—
6	0354	0.1	—	—

Sample No.	Time	Dye (ppb)	Dissolved PO_4 (ppb)	Chloride (ppm)
Sampler D—Continued				
8	0542	0.1	—	—
10	0730	0.1	—	—
12	0918	0.1	—	—
13	1012	0.0	—	—
14	1106	0.1	—	—
15	1200	0.1	—	—
16	1254	0.0	—	—
17	1348	0.1	—	—
18	1442	0.1	—	—
19	1536	0.1	—	—
20	1630	0.0	—	—
21	1724	0.0	—	—
22	1818	0.1	—	—
D2-1	1924	0.1	0	20.4
2	2018	0.1	3	20.4
3	2112	0.1	19	21.1
4	2206	0.1	27	20.6
5	2300	0.1	43	21.3
6	2354	0.1	43	21.1
	8/12/80			
7	0048	1.7	51	22.3
8	0142	0.6	19	20.1
9	0248	1.2	59	20.8
10	0330	0.6	59	21.1
11	0424	1.1	75	21.3
12	0518	0.2	131	19.9
13	0612	0.5	123	19.4
14	0706	0.3	171	19.7
15	0800	0.2	187	19.7
16	0854	0.3	163	19.7
17	0948	0.2	115	19.9
18	1042	0.2	139	19.7
19	1136	0.9	131	19.9
20	1230	1.2	115	21.1
21	1324	3.8	115	23.0
22	1418	3.6	128	22.7
23	1512	2.8	139	21.6
D3-1	1630	2.0	13	20.8
2	1724	2.1	23	20.6
3	1818	2.8	34	20.4
4	1912	1.6	23	19.7
5	2006	1.8	34	20.1
6	2100	0.8	44	19.4
7	2154	0.6	44	19.4
8	2248	0.4	39	18.8
9	2342	0.8	55	19.7
	8/13/80			
10	0048	1.7	39	21.1
11	0130	1.8	55	21.1
12	0224	1.7	86	21.8
13	0318	1.4	97	20.8
14	0412	1.8	65	21.3
15	0506	1.7	65	20.4
16	0600	1.5	—	20.7
17	0654	1.2	112	19.7
18	0748	1.2	97	19.0
19	0842	1.0	81	19.4
20	0936	0.8	70	18.8
21	1030	0.7	60	19.2
22	1124	1.3	60	19.9
D4-1	1248	1.2	13	21.1
2	1342	1.2	8	21.1
3	1436	1.2	3	20.8
4	1530	1.2	8	19.9
5	1624	1.2	3	20.1
7	1812	1.2	3	21.5
8	1906	1.3	8	20.8
9	2000	1.1	8	19.9
10	2054	0.9	13	22.7
11	2148	0.8	8	19.6
12	2242	0.8	8	19.2
13	2336	1.3	34	19.9
	8/14/80			
14	0030	1.3	40	20.8
15	0124	1.3	29	20.6
16	0218	1.2	66	21.3
17	0312	1.2	61	21.8
18	0406	1.2	40	21.5
19	0500	1.2	61	21.5
20	0554	1.2	55	21.5
21	0648	1.1	66	19.7
22	0742	1.1	61	20.8
D5-1	1000	0.3	—	—
2	1200	0.2	—	—
3	1400	0.4	—	—
4	1600	0.4	—	—
5	1800	0.3	—	—
6	2000	0.3	—	—
7	2200	0.3	—	—
8	2400	0.2	—	—
	8/15/80			
9	0200	0.3	—	—
10	0400	0.3	—	—
11	0600	0.2	—	—
12	0800	0.3	—	—
14	1200	0.2	—	—
16	1600	0.2	—	—
18	2000	0.2	—	—
20	2400	0.2	—	—
	8/16/80			
22	0400	0.2	—	—
24	0800	0.2	—	—
Sampler E				
	8/11/80			
E1-2	0018	0.0	—	—
4	0206	0.1	—	—
6	0354	0.0	—	—

Sample No.	Time	Dye (ppb)	Dissolved PO_4 (ppb)	Chloride (ppm)
		Sampler E — Continued		
8	0548	0.0	—	—
10	0736	0.1	—	—
12	0924	0.1	—	—
14	1118	0.1	—	—
16	1306	0.0	—	—
18	1454	0.1	—	—
20	1648	0.0	—	—
22	1836	0.0	—	—
E2-1	1930	0.1	31	20.4
2	2024	0.1	—	—
3	2118	0.7	21	20.8
4	2212	0.1	10	22.2
5	2306	0.1	21	20.7
	8/12/80			
6	0006	0.5	26	19.9
7	0100	0.3	21	22.2
8	0154	0.2	26	21.9
9	0248	0.3	26	21.0
10	0342	0.6	21	21.0
11	0424	0.4	36	21.0
12	0530	0.3	47	19.6
13	0630	0.2	57	19.3
14	0724	0.2	41	19.6
15	0818	0.2	36	18.7
16	0912	0.2	21	19.3
17	1006	0.2	26	19.0
18	1106	0.4	36	20.1
19	1200	0.2	31	19.9
20	1254	0.6	41	20.4
21	1348	0.8	41	21.6
22	1442	0.9	41	21.3
23	1536	1.5	52	21.6
E3-1	1618	0.5	18	21.0
2	1712	1.7	18	20.7
3	1806	1.3	28	21.0
4	1900	0.8	39	19.9
5	1954	0.4	23	19.3
6	2048	0.3	18	20.1
7	2148	0.2	13	19.6
8	2242	0.3	18	20.1
9	2336	0.3	—	19.0
	8/13/80			
10	0030	0.3	28	19.6
11	0124	1.5	34	21.0
12	0218	1.7	39	22.2
13	0318	1.5	44	21.6
14	0412	1.3	55	21.3
15	0506	1.2	102	18.7
16	0600	1.2	102	19.0
17	0654	1.0	86	20.4
18	0748	0.6	70	19.6
19	0848	0.4	55	20.4
20	0942	0.4	44	18.7
21	1036	0.3	39	19.6
22	1130	0.5	24	21.0

Sample No.	Time	Dye (ppb)	Dissolved PO_4 (ppb)	Chloride (ppm)
		Sampler E — Continued		
E3-1	1230	0.8	8	21.6
2	1324	1.5	13	21.6
3	1418	1.6	13	22.5
4	1512	1.3	8	21.3
5	1606	1.2	3	20.1
6	1700	1.1	8	21.6
7	1800	1.1	8	21.6
8	1854	1.1	40	19.9
9	1948	1.2	24	21.0
10	1042	1.0	18	20.1
11	2136	0.8	8	20.4
12	2230	0.6	8	20.1
13	2330	0.7	8	20.4
	8/14/80			
14	0024	1.1	24	20.7
15	0118	0.8	18	19.6
16	0212	0.8	29	20.4
17	0306	1.1	40	21.0
18	0400	1.2	24	21.0
19	0500	1.3	24	21.6
20	0554	1.3	18	21.9
21	0648	1.0	76	19.3
22	0742	1.1	71	20.1
23	0848	1.0	18	20.1
24	0930	0.8	13	19.6
E5-1	1200	0.3	—	—
2	1400	0.1	—	—
3	1600	0.2	—	—
4	1800	0.3	—	—
5	2000	0.3	—	—
6	2200	0.3	—	—
7	2400	0.2	—	—
	8/15/80			
8	0200	0.2	—	—
9	0400	0.2	—	—
10	0600	0.3	—	—
11	0800	0.2	—	—
12	1000	0.2	—	—
13	1200	0.2	—	—
14	1400	0.2	—	—
15	1600	0.2	—	—
16	1800	0.3	—	—
17	2000	0.2	—	—
18	2200	0.2	—	—
19	2400	0.2	—	—
	8/16/80			
20	0200	0.2	—	—
21	0400	0.2	—	—
22	0600	0.2	—	—
23	0800	0.2	—	—
24	1000	0.1	—	—

Sample No.	Time	Dye (ppb)	Dissolved PO_4 (ppb)	Chloride (ppm)
Sampler F				
	8/11/80			
F2–1	1963	0.2	31	20.5
5	2324	0.1	10	16.1
	8/12/80			
10	0406	0.1	31	16.4
15	0848	0.1	16	14.9
20	1330	0.3	62	16.1
24	1712	0.4	52	20.7
F3–3	1800	0.6	18	16.1
5	1948	0.3	28	15.7
7	2142	0.2	28	15.9
9	2336	0.1	28	15.7
	8/13/80			
11	0130	0.7	44	15.7
13	0318	0.6	60	16.8
15	0512	1.0	97	15.1
17	0706	1.0	97	17.5
19	0900	0.4	49	15.5
21	1054	0.1	39	15.5
F4–1	1230	1.0	13	16.1
3	1400	1.2	18	15.7
5	1548	1.3	8	17.0
7	1742	1.3	8	16.6
9	1936	1.2	3	15.9
11	2130	0.9	13	17.2
13	2318	0.6	13	18.8
	8/14/80			
15	0112	1.1	13	19.1
17	0306	1.2	13	17.0
19	0500	1.1	24	17.2
21	0654	1.1	71	15.7
23	0842	1.0	45	17.5
F5–1	0930	0.2	—	—
3	1330	0.3	—	—
5	1730	0.3	—	—
7	2130	0.3	—	—
	8/15/80			
9	0130	0.3	—	—
11	0530	0.3	—	—
13	0930	0.3	—	—
15	1330	0.3	—	—
17	1730	0.3	—	—
19	2130	0.2	—	—
	8/16/80			
21	0130	0.2	—	—
23	0530	0.1	—	—